Oxidation of cetirizine, fexofenadine and hydrochlorothiazide during ozonation: Kinetics and transformation products

Ewa Borowska [a,b], Marc Bourgin[a], Juliane Hollender [a,c], Cornelia Kienle [d], Christa S. McArdell [a*], Urs von Gunten [a,c,e*]

[a] Eawag, Swiss Federal Institute of Aquatic Science and Technology, CH-8600 Dübendorf, Switzerland

[b] Silesian University of Technology, Faculty of Power and Environmental Engineering, Environmental Biotechnology Department, PL-44100 Gliwice, Poland

[c] Institute of Biogeochemistry and Pollutant Dynamics (IBP), ETH Zurich, CH-8092 Zurich, Switzerland

[d] Swiss Centre for Applied Ecotoxicology Eawag-EPFL, Überlandstrasse 133, CH-8600 Dübendorf, Switzerland

[e] School of Architecture, Civil and Environmental Engineering (ENAC), Ecole Polytechnique Fédérale de Lausanne (EPFL), CH-1015 Lausanne, Switzerland

* Corresponding authors: Christa S. McArdell, phone +41 58 765 5483; fax +41 58 765 5028, email: christa.mcardell@eawag.ch, Urs von Gunten, phone: +4158 765 5270, fax: +41 58 765 5210, email: urs.vongunten@eawag.ch.

The published version is available at:
Borowska, E., Bourgin, M., Hollender, J., Kienle, C., McArdell, C. S., & Von Gunten, U. (2016). Oxidation of cetirizine, fexofenadine and hydrochlorothiazide during ozonation: kinetics and formation of transformation products. Water Research, 94, 350-362. http://doi.org/10.1016/j.watres.2016.02.020

Abstract

The efficiency of wastewater ozonation for the abatement of three nitrogen-containing pharmaceuticals, two antihistamine drugs, cetirizine (CTR) and fexofenadine (FXF), and the diuretic drug, hydrochlorothiazide (HCTZ), was investigated. Species-specific second-order rate constants for the reactions of the molecular, protonated (CTR, FXF) or deprotonated (HCTZ) forms of these compounds with ozone were determined. All three compounds are very reactive with ozone (apparent second order rate constants at pH 7: $k_{O3,pH7}$ = $1.7 \cdot 10^5$ $M^{-1}s^{-1}$, $8.5 \cdot 10^4$ $M^{-1}s^{-1}$ and $9.0 \cdot 10^3$ $M^{-1}s^{-1}$ and, for CTR, HCTZ and FXF, respectively). Transformation product (TP) structures were elucidated using liquid chromatography coupled with high-resolution tandem mass spectrometry, including isotope-labeled standards. For cetirizine and hydrochlorothiazide 8 TPs each and for fexofenadine 7 TPs were identified. The main TPs of cetirizine and fexofenadine are their respective *N*-oxides, whereas chlorothiazide forms to almost 100% from hydrochlorothiazide. In the bacteria bioluminescence assay the toxicity was slightly increased only during the ozonation of cetirizine at very high cetirizine concentrations. The main TPs detected in bench-scale experiments were also detected in full-scale ozonation of a municipal wastewater, for >90% elimination of the parent compounds.

Key words: ozonation, second-order rate constant, kinetics, transformation products, high-resolution mass spectrometry

1. Introduction

Ozone-based processes for the abatement of micropollutants have been studied intensively in bench-scale (Acero et al. 2000, Dantas et al. 2007, Garoma et al. 2010, Mawhinney et al. 2012, McDowell et al. 2005), pilot-scale (Gerrity et al. 2011, Huber et al. 2005, Lajeunesse et al. 2013, Margot et al. 2013) and a few full-scale systems (Hollender et al. 2009, Nakada et al. 2007) indicating the huge potential of these methods. Unfortunately, ozonation does not cause full mineralization and therefore transformation products (TPs) are formed (von Sonntag and von Gunten 2012). Literature concerning biodegradability of ozonation products is limited, but it is assumed that introduction of oxygen atoms in the molecules potentially leads to an increased biodegradability (Hübner et al. 2015). Therefore, it is often recommended to add biological post-treatment such as sand filtration after ozonation of wastewater effluents (Hollender et al. 2009, Zimmermann et al. 2011). For instance, Hübner and co-workers showed that the primary ozone transformation product of carbamazepine was more effectively biodegraded in sand columns than the parent compound (Hübner et al. 2014). However, as recently concluded in a review, especially oxidation products of nitrogen containing compounds such as *N*-oxides and hydroxylamines are not better biodegradable than the parent compounds (Hübner et al. 2015). Therefore, there is a need for the elucidation of structures of ozonation TPs and their potential ecotoxicological impact on the aquatic environment (Bourgin et al. 2013, Carbajo et al. 2015).

Because ozonation is already used in drinking water treatment and also increasingly in wastewater treatment for micropollutant abatement, detailed knowledge on the kinetics of micropollutant abatement and the formation of TPs is essential. To this end, there is already significant information in literature, which allows to estimate the abatement of selected compounds during wastewater ozonation (von Sonntag and von Gunten 2012). However, with the discovery of new classes of compounds, there is a need for more information on their behavior during ozonation.

This study concentrates on cetirizine and fexofenadine, two antihistamine drugs used for the treatment of allergic reactions, and hydrochlorothiazide - a diuretic drug commonly used in the treatment of hypertension. These compounds are frequently detected in municipal wastewater effluents and natural aquatic systems (Al-Qaim et al. 2014, Bahlmann et al. 2012, Kosonen and Kronberg 2009, Oosterhuis

et al. 2013). Cetirizine was found in wastewater effluents in Germany in concentrations of up to 510 ng L^{-1} (Bahlmann et al. 2012), in river water in Finland in concentrations of up to 9 ng L^{-1} (Kosonen and Kronberg, 2009) and in the San Francisco Bay and the Baltic Sea (German coast line) in concentrations of up to 6 and 13 ng L^{-1} (Nödler et al. 2014). In an extreme case, cetirizine was detected in concentrations of up to 1.2 mg L^{-1} in lake water, in an area with pharmaceutical industry in India (Fick et al. 2009). Fexofenadine was found in municipal wastewater effluent in Finland at a maximum concentration of 100 ng L^{-1}, and its elimination during a biological process was calculated to be 18% (Kosonen and Kronberg 2009). In river water up to 11 ng L^{-1} fexofenadine were measured (Kosonen and Kronberg 2009). Hydrochlorothiazide was detected in very high frequency (>85%) in high concentrations (hundreds of ng L^{-1} to 17.2 μg L^{-1}) in municipal wastewater samples in the Netherlands (Oosterhuis et al. 2013), Spain (Bueno et al. 2012) and Canada (Kim et al. 2014) and the elimination of this compound was demonstrated to be incomplete (0-77%) during conventional biological wastewater treatment (Castiglioni et al. 2006). Hydrochlorothiazide was detected at low ng L^{-1} levels (up to 54 ng L^{-1}) in Malaysian river waters (Al-Qaim et al. 2014).

Information on effects of these substances is scarce. For cetirizine hydrochloride, an EC_{50} of 330 mg L^{-1} was reported for the water flea *Daphnia magna* (Webb 2001) and a 96-h LC_{50} for the flatworm *Dugesia japonica* of 209.5 mg L^{-1} (Li 2013). The lowest concentration causing toxicity of fexofenadine hydrochloride was estimated to be 0.387 mg L^{-1} for *Daphnia magna* and 114 mg L^{-1} for fish (based on ECOSAR Data) (Sanderson et al. 2004). Hydrochlorothiazide elicited effects on algae growth with a 72-h EC_{50} of 34.35 mg L^{-1} (Fernández et al. 2010), whilst the 5-d LC_{25} for zebrafish embryos and larvae was above 1000 μM (300 mg L^{-1}) (Gustafson et al. 2012). However, there is no information concerning effects of their transformation products.

All three pharmaceuticals, cetirizine, fexofenadine and hydrochlorothiazide (Fig. 1), are nitrogen-containing compounds. Cetirizine and fexofenadine contain tertiary amine moieties whereas hydrochlorothiazide has an aniline-like moiety within a saturated ring structure and two sulfonamide groups. According to the pK_a-values recorded in literature, differently charged nitrogen species occur under environmental conditions. This is especially relevant as only the non-protonated nitrogen atoms exhibit enough electron density to react with ozone (von Sonntag and von Gunten 2012). Due to their

94 occurrence in wastewater effluents, the expected high reactivity with ozone and the possible formation
95 of recalcitrant TPs such as *N*-oxides, the three compounds were selected to assess their fate during
96 ozonation. The kinetics of the reaction of ozone with the target compounds and some identified TPs
97 were investigated over a wide pH range to determine species-specific second-order rate constants.
98 Additionally, TPs formed during ozonation were identified by liquid chromatography coupled with
99 high-resolution tandem mass spectrometry to propose reaction mechanisms. Potential ecotoxicological
100 effects of the compounds and their TPs on bacteria were assessed with a bacteria luminescence
101 inhibition assay. The abatement of the selected compounds and the formation of TPs were also
102 investigated in wastewater during full-scale ozonation.

103 **2. Material and methods**

104 **2.1. Chemicals and reagents**

105 All chemicals used in the study were of the highest purity available (Supplementary Information (SI)
106 Text S1). Ozone stock solutions were prepared as described in Text S2.

107 **2.2. Measurement of reaction kinetics**

108 *2.2.1 Ozonation experiments*

109 All kinetic experiments were carried out at 20±2 ºC. Apparent second-order rate constants k_{O3} for the
110 reaction of cetirizine, fexofenadine and hydrochlorothiazide (initial concentration 70 µM) with ozone
111 were determined using competition kinetics (Muñoz and von Sonntag 2000a, von Sonntag and von
112 Gunten 2012) with *trans*-cinnamic acid, *p*-cresol, 1-penten-3-one, 1,4-benzoquinone or orotic acid as
113 competitors (initial concentration 100 µM) (Table S1, Text S3). Kinetic experiments for cetirizine
114 were performed in the pH range 2-11, for fexofenadine in the pH range 7-12, and for
115 hydrochlorothiazide in the pH range 2-12. The pH of the solutions was kept constant by a 40-50 mM
116 phosphate buffer adjusted by 1 M HCl or 1 M NaOH. To verify the buffer capacity, the pH was also
117 measured in ozonated samples and a deviation of <0.1 pH unit was observed. Reactions of hydroxyl
118 radicals ($^{\bullet}$OH) were suppressed by addition of 20-100 mM *tert*-butanol (*t*-BuOH) used as $^{\bullet}$OH
119 scavenger. Similarly, k_{O3} values for highly reactive TPs (cetirizine *N*-oxide, norchlorcyclizine and
120 azacyclonol) were determined at pH 7, using competition kinetics as described above. Second-order
121 rate constants for TPs with low ozone reactivity - 4-chlorobenzophenone, fexofenadine *N*-oxide and

chlorothiazide - were determined under pseudo-first order conditions (Yao and Haag 1991), using ≥ 20-fold excess of ozone relative to the target compound. Further information about this method is given in Text S4.

2.2.2. Analysis by HPLC-DAD

The residual concentrations of the target compounds during kinetic experiments were measured by high performance liquid chromatography with a diode-array detector HPLC-DAD (UltiMate3000, Dionex) using an Atlantis® T3 3µm 3.0 x 150 mm column (Waters). A gradient program was applied with 0.1% formic acid in nanopure water (NPW) and acetonitrile for cetirizine and hydrochlorothiazide and their TPs. Fexofenadine was analyzed using a modified method described elsewhere (Vaghela et al. 2012), with 0.05% triethylamine in NPW and acetonitrile as mobile phases. For information about detection wavelengths and gradient programs see Table S3.

2.3. Identification of TPs

2.3.1. Sample preparation

The experimental solution contained 40 µM of a target compound. $^{\bullet}$OH were scavenged using 100 mM of *t*-BuOH. The solutions were buffered with 50 mM phosphate at pH 7. The experimental mixtures were ozonated by addition of an aliquot of the ozone stock solution to achieve varying ozone:target compound molar ratios, ranging from an excess of compound (ratio=0.1) to an excess of ozone (ratio=10). The analyses were performed after complete depletion of ozone. Additionally, as a control, non-ozonated samples were prepared, for which the ozone stock solution was replaced by NPW.

2.3.2. Identification of TPs by LC- HRMS/MS

Separation of TPs was achieved with an Atlantis® T3 3µm 3.0 x 150 mm column (Waters). Analytes were eluted with a gradient program using MeOH and water, both acidified with 0.1% formic acid. MS data were acquired by a ThermoScientific™ Q-Exactive™ Hybrid Quadrupole-Orbitrap Mass Spectrometer. MS data were collected in parallel full scan mode (60-700 m/z) at 70'000 resolution, using both positive and negative electrospray ionization. Data were analyzed with Xcalibur™ (Thermo Scientific™, Switzerland) in the Qual Browser. Before injection, samples were spiked with the internal standard of the parent compounds - CTR-d_8, FXF-d_6 or HCTZ-^{13}C,d_2 (Fig S4) - for the

150 calculation of normalized area, *i.e.* the ratio between the peak area of the analyte of interest and the
151 peak area of the internal standard of the corresponding parent compound. To obtain MS^2 spectra of the
152 potential TPs, ozonated samples were re-analyzed with the same analytical method, and using different
153 collision energies to reveal all relevant signals of the structure fragments. Values of HCD (Higher-
154 energy collisional dissociation) were in the range 10-70 %.
155 Detailed information about analytical conditions are presented in Table S4.
156 *2.3.3. Non-target screening*
157 The search for unknown TPs was performed by differential analysis. The collected full-scan MS
158 spectra of ozonated samples were analyzed by the SIEVE™ Thermo Scientific software. Non-spiked,
159 ozonated water and non-ozonated solutions of the compounds served as the control samples. By
160 comparison of treated samples (spiked and ozonated) with control samples, the peaks potentially
161 corresponding to TPs were selected. MS^2 spectra of detected peaks were subsequently acquired to
162 propose the structure of TPs.
163 *2.3.4. Structural confirmation by comparison with ozonated labeled compounds*
164 The labeled compounds cetirizine-d_8 and hydrochlorothiazide-$^{13}C,d_2$ (Fig. S4) were ozonated using the
165 same protocol as for non-labeled compounds. The comparison of the MS and MS^2 spectra for TPs
166 formed from labeled and non-labeled compounds, especially the comparison of signal shifts caused by
167 the labeled atoms, can provide additional evidence for the possible structure.
168 **2.4. Quantification and ecotoxicological evaluation of formed TPs in bench-scale experiments**
169 For the quantification of commercially available TPs, solutions containing the parent compounds
170 (CTR, FXF and HCTZ) at a concentration of 35 µM, buffered at pH 7 (50 mM phosphate buffer) were
171 ozonated. $^{\bullet}OH$ were scavenged using 100 mM *t*-BuOH. Aliquots of ozone stock solution were added
172 to reach ozone:target compound ratios of 0.1, 0.2, 0.5, 1, 2, 5, 10 and 20. Compounds (parent
173 compounds and their TPs) were quantified using LC-HRMS (Table S5). Additionally,
174 ecotoxicological effects of samples without ozone and with ozone:target compound ratios of 1, 5, and
175 20 on bacteria were assessed in a bacteria luminescence inhibition assay as described in SI Text S7.
176 **2.5. Determination of the yields of $^{\bullet}OH$ and chlorothiazide during hydrochlorothiazide**
177 **ozonation.**

178 To pH 7-buffered solutions of hydrochlorothiazide (1.6 µmol HCTZ in 8 mL NPW with an excess of
179 *t*-BuOH, *i.e.* 400 mM), an amount of 0.07-1.07 µmol ozone was dosed. Under these conditions, $^{\bullet}OH$
180 reacts preferentially (>99.5%) with *t*-BuOH ($k_{\cdot OH} = 6 \cdot 10^8$ M^{-1} s^{-1}) compared to hydrochlorothiazide
181 ($k_{\cdot OH} = 5.7 \cdot 10^9$ M^{-1} s^{-1}) (Real et al. 2010). The $^{\bullet}OH$ yield was directly determined by quantifying the
182 formation of formaldehyde. Two moles of $^{\bullet}OH$ are produced per mole of formaldehyde (Nöthe et al.
183 2009). HCTZ and chlorothiazide were quantified using the HPLC-DAD method described in Table
184 S6.

185 **2.6. Analysis of wastewater samples from a full-scale ozonation reactor**

186 The efficiency of ozonation for CTR, FXF and HCTZ abatement was investigated in a full-scale
187 ozonation facility (WWTP Neugut, Dübendorf, Switzerland, population equivalent 105'000) using 4
188 ozone doses (specific ozone doses), namely, 2 g O_3 m^{-3} (0.35 g O_3 g^{-1} DOC), 3 g O_3 m^{-3} (0.54 g O_3 g^{-1}
189 DOC), 4 g O_3 m^{-3} (0.67 g O_3 g^{-1} DOC) and 5 g O_3 m^{-3} (0.97 g O_3 g^{-1} DOC). Three flow proportional
190 24-h composite samples on three consecutive dry days were taken from two sampling points: (i) after
191 the secondary clarifier (O_3-INF) and (ii) after the ozone reactor (O_3-EFF). Samples were filtered
192 through two layers of Whatman® glass microfiber filters (bottom layer: GF/F, pore size 0.7 µm, top
193 layer: GF/D, pore size 2.7 µm). To improve the extraction efficiency and reduce matrix interferences,
194 the wastewater samples were diluted with NPW (4-fold for the O_3-INF and 2-fold for the O_3-EFF). All
195 samples were spiked with internal standards (cetirizine-d_8, fexofenadine-d_6, hydrochlorothiazide-
196 $^{13}C,d_2$) and analyzed using online solid-phase extraction coupled to the same LC-HRMS described
197 above (online-SPE LC-HRMS). The analytical method used for the measurement is described
198 elsewhere (Jeon et al. 2013).

199 **3. Results and discussion**

200 **3.1. Kinetic experiments**

201 *3.1.1. Reactivity of cetirizine with ozone*

202 Cetirizine contains two tertiary amines (Fig. 1a), which are expected to react with ozone. The pK_a
203 values have previously been determined (Tam and Quere 2001) as 2.1 (pK_{a1}), 2.9 (pK_{a2}) and 8.0

204 (pK_{a3}), corresponding to the tertiary amine close to the biphenyl moiety (*N1*), the carboxylic group and
205 a tertiary amine next to the aliphatic chain (*N2*), respectively.
206 At low pH (2-5) no significant change of reactivity was observed (Fig. 1a). In this pH range mainly the
207 *N1*-non-protonated, *N2*-protonated form of CTR is present (Fig. 1a CTR_{PROT}). However, in contrast to
208 a prediction based on the reported pK_{a1} value, which suggests the presence of 50% of *N1,N2*-
209 diprotonated CTR at pH 2 (Fig.1a CTR_{DIPROT}), we did not observe a decrease of the apparent second-
210 order rate constant at pH 2. This might be an indication that the actual pK_{a1} value is lower than the
211 reported one. Based on the data at pH < 5 a second order rate constant for the reaction of the CTR_{PROT}
212 can be estimated as $(6.0\pm0.1)\cdot10^3$ M^{-1} s^{-1} (Table 1). At pH>5, the reactivity of cetirizine with ozone
213 increases due to the presence of the molecular form of *N2*-amine (Fig. 1a CTR_{MOL}), which is assumed
214 to be the most reactive site of CTR. The apparent second-order rate constant for the reaction of CTR
215 with ozone increased to a value of $(1.7\pm0.1)\cdot10^5$ M^{-1} at pH 7 (Fig. 1a, Table 1). The species-specific
216 rate constant of CTR_{MOL} was determined as $2.8\cdot10^5$ M^{-1} s^{-1} (Text S5), which is comparable with the
217 experimental values at pH 9 ($(2.8\pm0.1)\cdot10^5$ M^{-1} s^{-1}) and pH 11 ($(3.4\pm0.1)\cdot10^5$ M^{-1} s^{-1}).
218 The obtained k_{O3} values for the reaction of CTR with ozone are comparable to other non-protonated
219 tertiary amines such as tramadol ($1.0\cdot10^6$ $M^{-1}s^{-1}$) and tylosin ($2.7\cdot10^6$ $M^{-1}s^{-1}$) (Dodd et al. 2006,
220 Zimmermann et al. 2012).
221 The data in Fig. 1a were fitted (line) with a pK_{a3} = 7.0 for the *N2* tertiary amine, which is lower than
222 the previously reported pK_{a3} of 8.0 (Tam and Quere 2001). Our kinetic data from a large pH range
223 point clearly towards this lower pK_a value of the *N2* tertiary amine group (Text S5, Fig. S1a).
224 *3.1.2. Reactivity of fexofenadine with ozone*
225 Fexofenadine contains a tertiary amine group, which is the most probable site of ozone attack. The pK_a
226 values reported for fexofenadine are 4.2 and 9.5, for the carboxylic and the amine group, respectively
227 (Ming et al. 2011, Yasui-Furukori et al. 2005). The carboxylic group is not relevant for ozone attack,
228 wherefore the FXF reactivity with ozone was investigated only in the pH range 7-12 (Fig. 1b). The k_{O3}
229 value determined at pH 12 for fexofenadine was $(5.7\pm0.1)\cdot10^5$ M^{-1} s^{-1} (Table 1), which is in agreement
230 with the value of $5.6\cdot10^5$ M^{-1} s^{-1} obtained for the species-specific rate constant of the molecular form of
231 FXF (Fig. 1b FXF_{MOL}, Text S5). The data suggests that the pK_a value of the amine group of

fexofenadine is lower than previously reported. The determined apparent second-order rate constants shown in Fig. 1b were better modeled by a pK_a of 9.0 (Fig. S1b), which is below the previously reported value of 9.5 (Ming et al. 2011, Yasui-Furukori et al. 2005). It has to be emphasized that in none of these publications, any details on the determination of the pK_a values were provided.

At pH 7 k_{O3} of FXF was determined as $(9\pm0.1)\cdot10^3$ M^{-1} s^{-1} (Table 1). At this pH, 1% of FXF is still in molecular form (assuming a pK_a of 9.0), contributing strongly to the k_{O3} value. k_{O3} for the protonated FXF (Fig. 1b FXF_{PROT}) should be considerably lower when comparing to other protonated tertiary amines (e.g k_{O3} = 77 $M^{-1}s^{-1}$ for tramadol (Zimmermann et al. 2011), 5 $M^{-1}s^{-1}$ for triethylamine (Pryor et al. 1984).

3.1.3. Reactivity of hydrochlorothiazide with ozone

Hydrochlorothiazide contains one aniline-like moiety and two sulfonamide (cyclic and free) groups (Fig. 1c). The free sulfonamide group (S^2) does not react with ozone (von Sonntag and von Gunten 2012). The reported pK_a values of hydrochlorothiazide show considerable variability (Hennig et al. 1981, Mollica et al. 1971, Vujić et al. 2012). The pK_a of aniline (Ph-NH_2/$PhNH^-$) was reported to be in the range 9.0-11.0 while the pK_a of the cyclic sulfonamide (R-SO_2NH_2/R-SO_2NH^-) was estimated to be in the range of 6.5-8.5.

Apparent second-order rate constants for the reaction of hydrochlorothiazide with ozone were determined in the pH range 2-12. At pH>11, apparent second-order rate constants remained constant at $(5.1\pm0.1)\cdot10^5$ M^{-1} s^{-1} (Fig. 1c $HCTZ_{DIDEPROT}$), reflecting the rate constants of the completely deprotonated molecule (both the sulfonamide and the aniline-like moiety are deprotonated; Table 1). From pH 11 to pH 8, the apparent second-order rate constants decreased by a factor of 2 to a value of $\sim3\cdot10^5$ M^{-1} s^{-1} (Fig. 1c), indicating that the protonation of the negatively-charged aniline moiety affects the reactivity of hydrochlorothiazide with ozone only slightly. At pH<8, the k_{O3} value decreased significantly to 590 (± 70) M^{-1} s^{-1} at pH<3.5, showing that a protonation of the N-atom in the cyclic sulfonamide group (S^1, Fig.1c $HCTZ_{MOL}$) contributes distinctly to the overall reactivity of hydrochlorothiazide with ozone. In a previous publication (Real et al. 2010) apparent second-order rate constants for the reaction of hydrochlorothiazide with ozone were determined at four pH values (3, 5, 7 and 9). However, the values they obtained were about one order of magnitude lower than the

values presented in this paper. The second-order rate constants reported in the aforementioned paper were determined using the competition method in a semi-batch reactor with metoprolol as a competitor. The complication with ozone mass transfer and the use of a different competitor might explain the discrepancies between the second order rate constants presented in both studies.

Based on the previous kinetic data, species specific second-order rate constants were calculated to be 590 (± 70) M^{-1} s^{-1} for the $HCTZ_{MOL}$, ~$3 \cdot 10^5$ M^{-1} s^{-1} for $HCTZ_{DEPROT}$ and 5.1 (±0.1)$\cdot 10^5$ M^{-1} s^{-1} for the $HCTZ_{DIDEPROT}$ (Fig. 1c, Table 1).

The pH dependence of the apparent second-order rate constants for the reaction of hydrochlorothiazide with ozone was best modeled by pK_a values of the cyclic sulfonamide (S^1) and the aniline moieties aof 7.0 and 10.5, respectively (Fig. 1c), which is in the range of the previously reported pK_a values.

Detailed results on the kinetics of HCTZ oxidation by ozone are compiled in the Table S2.

3.2. Identification of TPs

3.2.1. TPs of the reaction of cetirizine with ozone

Eight TPs of cetirizine ozonation were detected in the screening (Fig. 2a). As expected, the tertiary amine groups were the main sites of ozone attack. *N*-oxide formation has been previously reported for the reaction of tertiary amines with ozone (Muñoz and von Sonntag 2000b, Zimmermann et al. 2012). Due to the presence of two tertiary amines in the structure of cetirizine, *N*-oxidation may occur at two sites. Based on the information provided by MS^2 spectrum of CTR-TP1 (Fig. 2a), it was impossible to distinguish which *N*-oxide was formed. However, as discussed above, kinetic data showed that the *N2*-amine is more reactive than the *N1*-amine. Therefore cetirizine *N2*-oxide is more likely formed than *N1*-oxide. Additionally the available standard of cetirizine *N2*-oxide had a similar HPLC RT and MS^2 spectrum as CTR-TP1 (Fig. S11) which also confirmed the kinetics-based assumption about the structure of CTR-TP1.

The oxidation of CTR with higher ozone:CTR ratios resulted in the formation of a molecule with a *m/z* signal shifted by 15.995 Da from CTR-TP1, corresponding to an additional oxygen in the structure (CTR-TP5). A *N*-oxidation at the N1 position can be proposed, leading to the formation of CTR-*N,N'*-dioxide. This hypothesis was also supported by ozonation experiments with CTR-*N*-oxide as starting compound. While the signal of CTR-*N*-oxide decreased, the formation of CTR-TP5 (CTR-*N,N'*-

dioxide) was observed (Fig. S6). Alternatively to an *N*-oxidation, tertiary amines can undergo a dealkylation, though this reaction has generally a much lower efficiency (Zimmermann et al. 2012). Nevertheless, signals corresponding to dealkylated TPs were detected. A dealkylation of the tertiary amine groups resulted in the formation of a secondary amine and a carbonyl-containing molecule. In the case of cetirizine, a disruption of the C-N bond (position *N1*) resulted in the formation of CTR-TP2 (4-chlorobenzophenone, 4-CBP) and CTR-TP3 (Fig. 2a). The presence of CTR-TP2 could be confirmed by an available standard (Fig. S12). Furthermore, during the ozonation of CTR-d_8, a compound with a similar HPLC RT and the same *m/z* value as in the ozonated non-labeled CTR samples was observed, which confirmed that CTR-TP2 most likely contained the aromatic moiety of cetirizine. CTR-TP3, which contains one secondary amine and one tertiary amine group, can be further oxidized at the *N*-atoms to form the corresponding *N*-oxide (CTR-TP6) and/or a hydroxylamine (CTR-TP7) (*m/z* signal shift of 15.995 Da from CTR-TP3). Another TP (CTR-TP8) with an additional increase of the *m/z* value of 15.995 Da compared to CTR-TP6/7 was detected, suggesting formation of the corresponding *N*-oxide,*N*'-hydroxylamine (CTR-TP8, Fig. 2a). All these oxidative transformations were supported by observed signal shifts of 8.0509 Da in the CTR-d_8 TPs. Dealkylation at the *N2*-atom of cetirizine resulted in the formation of CTR-TP4 (norchlorcyclizine, NCC), which was also confirmed by comparison with a commercial standard (Fig. S13). This compound could be further oxidized at the tertiary amine group. However, the signal of CTR-TP4 was low, which could be explained by a transient character of this compound. A more detailed discussion about the significance of the different ozone reactions is provided in section 3.4. Detailed information on CTR-TPs is provided in Table S7. MS^2 spectra of CTR TPs without commercial standards are presented in Figs. S17-S20. A discussion about using labeled compounds for structure confirmation is presented in Text S8.

All TPs were proposed based on knowledge of ozonation mechanisms and classified by confidence levels according to Schymanski et al. (2014). CTR-TP1, CTR-TP2 and CTR-TP4 are assigned to confidence level 1 (confirmation with commercial standard), CTR-TP3, CTR-TP5 and CTR-TP8 have a confidence level 2b (probable structure based on MS^2 spectra interpretation, information from ozonation of labeled compound and experimental context), CTR-TP6 and CTR-TP7 have a confidence

316 level 3 (tentative candidates based on MS^2 spectra interpretation, information from ozonation of
317 labeled compound and experimental context).

318 *3.2.2. TPs of the reaction of fexofenadine with ozone*

319 Seven fexofenadine TPs were identified (Fig. 2b). One of the most prominent ozone TPs (FXF-TP1)
320 was found to be fexofenadine *N*-oxide (FXF-*N*-oxide). The structure was confirmed by comparison
321 with the commercial standard FXF-*N*-oxide (Fig. S14). A difference of 2.0158 Da in FXF-TP4
322 compared to FXF-TP1 could be explained by the oxidation of a hydroxyl group to a ketone (loss of
323 two hydrogen atoms). Further evidence for the formation of FXF-TP4 from FXF-TP1 is provided with
324 the ozonation of a standard of FXF-*N*-oxide by various ozone:target compound ratios (Fig. S8).
325 However, this reaction is very slow (von Sonntag and von Gunten 2012) and is rather unlikely to
326 happen under realistic ozonation conditions with ozone.

327 Apart from an *N*-oxidation, dealkylation of FXF was also observed. The disruption of the N-C bond in
328 the heterocycle resulted in the formation of FXF-TP2, for which the structure was confirmed by
329 comparison with a commercial standard (azacyclonol ACC, Fig. S15). FXF-TP2, as a secondary
330 amine, could be further oxidized yielding TPs with the *m/z* signal shifted by 15.995 Da (an additional
331 oxygen atom). For this signal, two TPs were proposed: FXF-TP5, a hydroxylamine, and FXF-TP6, a
332 molecule where the N-C bond is cleaved, with an aldehyde formation after ring opening. The second
333 transformation is less likely than hydroxylation. Data provided by the MS^2 spectrum of the signal
334 284.1644 *m/z* were not sufficient to confirm the structure of the corresponding TPs.

335 FXF-TP3, for which a primary amine was proposed, resulted from di-dealkylation of FXF. For FXF-
336 TP7, which contained an oxygen more than FXF-TP3, a hydroxylamine structure is proposed.
337 However, the formation of a primary amine is rather unlikely and has a minor relevance in comparison
338 to *N*-oxidation. This is discussed in more detail in section 3.4.

339 Detailed information about FXF TPs is presented in Table S7 and their structures are proposed based
340 on the knowledge of ozone chemistry. MS^2 spectra of FXF TPs without commercial standards are
341 presented in SI Fig. S21-S24. FXF-TP1 and FXF-TP2 belong to confidence level 1, whereas the rest
342 of the proposed TPs (FXF-TP3-TP7) correspond to level 3.

343 *3.2.3. TPs of the reaction of hydrochlorothiazide with ozone*

344 Screening provided information about eight TPs of hydrochlorothiazide for which structures were
345 proposed (Fig. 2c).
346 For HCTZ-TP1, chlorothiazide (CTZ) was proposed based on MS^2 spectra. The standard of
347 chlorothiazide showed the same HPLC RT and HRMS/MS spectra as HCTZ-TP1 (Fig. S16).
348 Chlorothiazide was already assumed to be formed from hydrochlorothiazide during photodegradation
349 (Brigante et al. 2005) and biotransformation in river sediments (Li et al. 2014).
350 During ozonation of hydrochlorothiazide, the $^{\bullet}OH$ yield was determined to be 37 ± 1% (Fig. 3).
351 Chlorothiazide formation was proposed to consist of two successive electron-transfer reactions (Fig.
352 4a). In this mechanism, considering the high selectivity of the reaction (> 99%, as described later in
353 the section 3.4.3.), 2 moles of ozone are consumed per mole of HCTZ removed, thereby producing 1
354 mole of chlorothiazide and 2 moles of $^{\bullet}OH$ from the decomposition of the ozonide radical anion ($O_3^{\bullet-}$)
355 and the reaction of ozone with superoxide ($O_2^{\bullet-}$) (reactions (1-4)).

356 $O_3^{\bullet-} \rightleftarrows O_2 + O^{\bullet-}$ (1)

357 $O^{\bullet-} + H_2O \rightleftarrows {}^{\bullet}OH + OH^-$ (2)

358 $HO_2^{\bullet} \rightleftarrows O_2^{\bullet-} + H^+$ (3)

359 $O_2^{\bullet-} + O_3 \rightleftarrows O_2 + O_3^{\bullet-}$ (4)

360 Considering the $^{\bullet}OH$ yield, the electron-transfer mechanism accounts only for about 18.5% of the
361 formed of CTZ. Another mechanism (81.5%) involving only one mole of ozone without $^{\bullet}OH$
362 production, is proposed by the formation of a hydroxylamine and the subsequent loss of a hydroxyl
363 ion to form the corresponding imine (oxygen transfer pathway, Fig.4b). Considering the respective
364 yield and the number of ozone molecules involved in each mechanism, 1.2 moles ozone should be
365 consumed per mole of HCTZ. However, Fig. 3 shows that 1.5 moles of ozone were consumed per
366 mole of HCTZ removed. The difference may be explained by a catalytic destruction of ozone by
367 nitrogen- and carbon-centered radicals as presented in Fig. 4a (von Sonntag and von Gunten, 2012).
368 The seven other hydrochlorothiazide TPs were also formed when chlorothiazide was ozonated.,
369 confirming that chlorothiazide is a key intermediate during hydrochlorothiazide ozonation (Fig. 2c).

370 The proposed chemical formula of HCTZ-TP2 differed from HCTZ-TP1 only by the loss of one
371 nitrogen and one hydrogen atom and by the addition of one oxygen atom (mass shift of *m/z* 0.9838).
372 HCTZ-TP2 was therefore suspected to be the sulfonate analogue of HCTZ-TP1. This assumption
373 could be confirmed by the MS^2 fragmentation of both compounds: while the HCD fragmentation of
374 HCTZ-TP1 induced the formation of a SNO_2^- fragment ion (*m/z* 77.96502), the formation of a SO_3^-
375 fragment ion (*m/z* 79.95686) was observed during the fragmentation of HCTZ-TP2.
376 HCTZ-TP3 differed from hydrochlorothiazide by the addition of one oxygen atom. Hydroxylation or
377 heteroatomic ring opening/amide formation were suspected to occur, to explain the formation of
378 HCTZ-TP3. Ozonation experiments were carried out with hydrochlorothiazide labeled on the
379 methylene bridge with one ^{13}C and two deuterium (HCTZ-$^{13}C,d_2$, Fig. S4c) atoms between the aniline
380 moiety and sulfonamide group (S^1). The resulting TP3 showed a mass shift of one ^{13}C and one
381 deuterium compared to non-labeled hydrochlorothiazide, indicating that the site of ozone attack was
382 located at the alkyl group. Therefore, a hydroxylation of the aromatic ring was ruled out in this case.
383 The MS^2 experiments showed the loss of CO (*m/z* 27.995) from the parent ion of HCTZ-TP3, further
384 pointing to the formation of an amide group.
385 Transformation product HCTZ-TP5 was formed by addition of 2 oxygen atoms and loss of 2 hydrogen
386 atoms compared to HCTZ-TP3. HCTZ-TP5 might be formed from the oxidation of the aromatic ring
387 in HCTZ-TP3 resulting in a 1,4-benzoquinone derivative (see Text S6, Fig. S2).
388 HCTZ-TP7 was proposed to be a compound with only 6 carbon atoms, instead of 7 carbons for
389 HCTZ-TP5. The ozonation of the non-labeled and the labeled HCTZ induced the formation of the
390 same compound as HCTZ-TP7, without any mass shift from the isotopes. Therefore, this result
391 confirmed that the carbon atom lost during the oxidation is the carbon at the heteroatomic ring.
392 In analogy to HCTZ-TP1 and HCTZ-TP2, the TPs HCTZ-TP4, HCTZ-TP6 and HCTZ-TP8a/b were
393 assumed to be the sulfonate analogues of HCTZ-TP3, HCTZ-TP5 and HCTZ-TP7, respectively.
394 Detailed information concerning identified HCTZ TPs is presented in Table S7 and their structures are
395 proposed based on the knowledge of ozone chemistry. HCTZ-TP1 was assigned to confidence level 1,
396 HCTZ-TP2 and HCTZ-TP3 have confidence level 2b, whereas the rest of the proposed TPs (HCTZ-

TP4- HCTZ-TP8a/b) correspond to level 3. MS^2 spectra of HCTZ TPs without commercial standards are presented in SI Fig. S25-S32.

3.3. Reactivity of TPs with ozone

3.3.1. Cetirizine TPs

Apparent second-order rate constants at pH 7 for the reaction of ozone with the TPs with available commercial standards were also determined (Table 1). For CTR-*N*-oxide (CTR-TP1, Fig. 2a) the apparent second-order rate constant of $(8.3\pm0.1)\cdot10^3$ $M^{-1}s^{-1}$ was determined, which is significantly lower than the corresponding rate constant for CTR ($(1.7\pm0.1)\cdot10^5$ $M^{-1}s^{-1}$). 4-chlorobenzophenone (CTR-TP2, Fig. 2a) has no ozone-reactive moieties (ketone and inactivated benzene rings), explaining its very low reactivity (k_{O3} = (0.40 ± 0.05) $M^{-1}s^{-1}$). The apparent second-order rate constant of NCC (CTR-TP4, Fig. 2a) at pH 7 was determined to be $(2.1\pm0.1)\cdot10^4$ $M^{-1}s^{-1}$, reflecting the reaction of ozone with a tertiary amine. At pH 7, the secondary amine is protonated, since the pK_a values corresponding to the tertiary and the secondary amine of NCC are predicted with the ChemAxon software (http://www.chemicalize.org) as 3.9 and 9.2, respectively.

3.3.2. Fexofenadine TPs

The apparent second-order rate constant for the reaction of ozone with FXF-*N*-oxide (FXF-TP1, Fig. 2b) at pH 7 was ~6.0 ± 2.0 $M^{-1}s^{-1}$ (Table 1). This value is substantially lower than for the parent compound ($k_{O3,FXF}$ = $(9.0\pm0.1)\cdot10^3$ $M^{-1}s^{-1}$). The apparent second-order rate constant at pH 7 for the reaction of ozone with ACC (FXF-TP2, Fig. 2b) containing a secondary amine was 350 ± 10 $M^{-1}s^{-1}$ (Table 1). This is in a similar range as apparent second-order rate constants for the reaction of protonated secondary amines with ozone at pH 7 (*e.g.*, metoprolol $2\cdot10^3$ $M^{-1}s^{-1}$, atenolol $1.7\cdot10^3$ $M^{-1}s^{-1}$, (Benner et al. 2008, Benner and Ternes 2009). The value of $k_{O3,ACC}$ is lower than $k_{O3,FXF}$, based on the fact that secondary amines are less reactive towards ozone than tertiary amines (von Sonntag and von Gunten, 2012).

3.3.3. Hydrochlorothiazide TPs

The k_{O3} of CTZ (HCTZ-TP1, Fig. 2c) at pH 7 was determined to be 1.5 ± 0.1 $M^{-1}s^{-1}$, whereas under the same conditions the k_{O3} of HCTZ is $8.5\cdot10^4$ $M^{-1}s^{-1}$ (Table 1). This difference of 5 orders of magnitude

indicates that the imine group in the chlorothiazide structure strongly deactivates this compound compared to hydrochlorothiazide.

3.4. Evolution of TPs at different ozone to target compound ratios

3.4.1. Evolution of cetirizine TPs

Complete depletion of CTR was observed for ozone:CTR molar ratios > 2 (Fig. 5a). CTR-*N*-oxide was the most prominent TP of cetirizine for ozone:CTR ratio ≤2. According to mass balance, CTR was completely converted into CTR-*N*-oxide and, to a lower extend, to 4-CBP, up to ozone:CTR ratio of 1. For a molar excess of ozone relative to cetirizine, the *N*-oxide decreased with the formation of other TPs as outlined above.

4-CBP (CTR-TP2) increased with increasing ozone:CTR ratios, however, less pronounced than CTR-*N*-oxide (CTR-TP1). At an ozone:CTR molar ratio of 10, 35% of the initial concentration of CTR was transformed into 4-CBP. The accumulation of 4-CBP is expected from its low apparent second-order rate constant at pH 7 (see above). In all ozonated samples, NCC (CTR-TP4) was below LOQ, which indicates that this branch of the ozonation pathway (dealkylation at the N-atom of the heterocycle) is not relevant.

Due to the lack of commercial standards the rest of CTR-TPs could only be determined semi-quantitatively, based on the normalized peak area of the TPs divided by the peak area of CTR-d_8. CTR-*N*-oxide oxidation led to the formation of CTR-*N,N'*-dioxide (CTR-TP5, Fig. S5, Fig. S6 see section 3.2.1.). While the normalized area of CTR-*N*-oxide decreased, the normalized area of CTR *N,N'*-dioxide (CTR-TP5) increased. This confirms that this TP belongs to a second generation of cetirizine TPs. In Fig. S5 the change of the normalized area of CTR-TP6/7 as a function of the O_3 dose is illustrated. In all samples its normalized area was low, which demonstrates that de-alkylation of CTR-*N*-oxide is a minor pathway compared to *N*-oxidation of the two tertiary amine moieties.

CTR-TP3 was formed 1:1 with the formation of 4-CBP (CTR-TP2) (Fig. 2a). In contrast to 4-CBP, CTR-TP3 was quite reactive with ozone leading quickly to the next generation of TPs, namely TP6/7 (Fig. S5), subsequently oxidized to CTR-TP8.

3.4.2 Evolution of fexofenadine TPs

Complete depletion of FXF was observed for ozone:FXF molar ratios ≥2 (Fig. 5b). Based on the mass balance, the formation yield of FXF-*N*-oxide from FXF was determined to be almost 100% up to an ozone:FXF ratio of 0.5. Additionally, based on the mass balance, other FXF TPs are formed at ozone:FXF ratios ≥0.5. Unfortunately, due to the lack of commercial standards, they could not be quantified.

For higher ozone:FXF ratios, FXF-*N*-oxide was further oxidized to the FXF-TP4 (see section 3.2.2), which could be determined semi-quantitatively (Fig. S7, Fig. S8). ACC (FXF-TP2) was not formed in high concentrations (< 1μM for all ozone:FXF ratios), which suggests that *N*-dealkylation in the heterocycle is a minor reaction pathway during ozonation. The normalized areas of the peaks corresponding to FXF-TP5 and FXF-TP6, which were proposed as ACC-TPs, were small (data not shown). Therefore, their formation is highly unlikely under realistic conditions. Similarly, semi-quantitative determinations of FXF-TP3 and FXF-TP7 showed that these compounds are formed to a negligible extent.

3.4.3. Evolution of hydrochlorothiazide TPs

Fig. 5c shows that a complete depletion of the hydrochlorothiazide was observed for ozone:HCTZ molar ratios ≥ 2 with an almost quantitative formation (>99%) of CTZ (HCTZ-TP1, Fig 3, inset). For ozone:HCTZ molar ratios >2 an abatement of CTZ was observed, suggesting that CTZ was further oxidized with the formation of a second generation of TPs. However, as shown above, this reaction was very slow (k_{O3}= 1.5±0.1 M^{-1} s^{-1} at pH 7) and is hence not relevant under realistic conditions. Additional ozonation experiments with CTZ as parent compound led to the formation of the 7 other identified TPs (Fig. 2, Fig. S10). As no standards are available for these TPs, only a semi-quantitative analysis was possible (see section 3.4.1) (Fig. S9). HCTZ-TP2, the second predominant HCTZ-TP, started to increase significantly for ozone:HCTZ ratios≥2, simultaneously with the decrease of chlorothiazide (HCTZ-TP1). This could indicate that HCTZ-TP2 was formed directly from CTZ (HCTZ-TP1, Fig. 2c). HCTZ-TP3 increased at the lowest ozone:HCTZ molar ratio (up to stoichiometric conditions), and subsequently decreased with increasing ozone doses, showing the relatively significant reactivity of this compound with ozone and the formation of the next generation

478 TPs. HCTZ-TPs 4-8 increased as a function of the ozone:HCTZ molar ratio, but their normalized areas
479 were very low, indicating that these reactions have minor relevance.

480 **3.5. Ecotoxicological effects of cetirizine, fexofenadine and hydrochlorothiazide and their TPs in**
481 **bacteria bioluminescence tests**

482 No effects of the parent compounds on bacteria luminescence were detected at 31-38 µM. Cetirizine
483 samples treated with ozone elicited biological effects on bacteria bioluminescence with a 50% effect
484 concentration of 10.2 µM CTR (initial concentration, 4.0 mg L^{-1}) and a 10% effect concentration of
485 1.1 µM (0.4 mg L^{-1}) at an ozone:CTR ratio of 5 (Fig. S3). Taking the results discussed in section 3.4.1
486 (Fig. 5a) for the high excess of ozone into account, no CTR or CTR-*N*-oxide was present anymore in
487 these samples. This could indicate that the observed toxicity was caused by 4-CBP or by other CTR
488 TPs, which could not be confirmed with commercial standards.
489 Ozone-treated fexofenadine and hydrochlorothiazide samples did not exceed a 10% inhibition at the
490 highest concentrations tested. This clearly indicates that parent compounds and the corresponding
491 transformation products are not harmful towards the tested bacteria. For all three compounds, the
492 effect concentrations are well above environmentally relevant concentrations in the ng L^{-1} or low µg L^{-1}
493 range (see introduction).
494 Additional bioluminescence tests were also performed on wastewater effluent, showing a decrease of
495 the toxicity of up to 71% after ozonation. These results are discussed in detail elsewhere (McArdell et
496 al., 2015).

497 **3.6. Determination of CTR, FXF, HCTZ and their TPs during ozonation of real wastewater**
498 **samples**

499 Analyses of wastewater samples from the WWTP Neugut (Switzerland) showed that the investigated
500 compounds of this study are not completely removed during activated sludge treatment. They are
501 present in the effluent of the secondary clarifier, at the influent to the ozone reactor (O_3-INF), at
502 average concentrations of approximately 50 ng L^{-1}, 150-500 ng L^{-1} and 1000 ng L^{-1} for CTR, FXF and
503 HCTZ, respectively (Table 2). As expected from their reactivity, ozonation resulted in significant
504 abatement of these compounds. A comparison of the concentration in a sample before (O_3-INF) and
505 after ozonation (O_3-EFF) showed that an application of a low ozone dose of 2.03±0.15 g O_3 m^{-3}

506 (0.35±0.02 g O_3 g^{-1} DOC) caused an elimination of 92%, 86% and 83% for CTR, HCTZ and FXF,
507 respectively (Table 2). This is in agreement with the observed apparent second-order rate constants at
508 circumneutral pH ($k_{O3,CTR} > k_{O3,HCTZ} > k_{O3,FXF}$). An increase of the ozone dose to 3.00±0.09 g O_3 m^{-3}
509 (0.54±0.05 g O_3 g^{-1} DOC) resulted in a higher elimination of 90-99% for all investigated compounds.
510 Concomitant to the abatement of the parent compounds, the formation of TPs was investigated. From
511 the three CTR-TPs confirmed with commercial standards in the laboratory studies, cetirizine *N*-oxide
512 (CTR-*N*-oxide), 4-chlorobenzophenone (4-CBP) and norchlorcyclizine (NCC), only CTR-*N*-oxide was
513 found at a low concentration (4±2 ng L^{-1}), only for the lowest ozone dose (Table 2). The formation
514 yield of CTR-*N*-oxide was lower than 10%, which is significantly lower than in the laboratory studies.
515 Higher ozone doses might have caused further oxidation of CTR-*N*-oxide to the dioxide and therefore
516 its concentration was below LOQ. A possible explanation for the absence of the TPs at higher ozone
517 doses is their reaction with $^{\bullet}$OH, which are formed from ozone decomposition (von Sonntag and von
518 Gunten 2012). This may lead to different products, which were not identified in the current study
519 where $^{\bullet}$OH were scavenged. The extent of direct reaction with ozone or oxidation by $^{\bullet}$OH is controlled
520 by the water matrix and has been discussed in the literature (Lee et al., 2013, Lee et al., 2014).
521 None of the other cetirizine TPs was detected in ozonated wastewater samples.
522 FXF-*N*-oxide was identified in ozonated wastewater at a concentration of 141 ng L^{-1} at an ozone dose
523 of 2.72±0.13 g O_3 m^{-3} (0.54±0.04 g O_3 g^{-1} DOC), corresponding to a yield of FXF-*N*-oxide formation
524 from FXF of ~35%. The other proposed TPs from above were not detected.
525 CTZ was already detected in the influent of the WWTP as it is also used as a pharmaceutical
526 compound, and at the O_3-INF an average concentration of 55 ng L^{-1} was still observed (Table 2). A
527 significant formation of CTZ in wastewater was observed during ozonation with a concentration of up
528 to 436 ± 13 ng L^{-1} in the O_3-EFF for the lowest ozone dose (2.03±0.15 g O_3 m^{-3} = 0.35±0.02 g O_3 g^{-1}
529 DOC) with a yield of about 40% from HCTZ. With increasing ozone doses, the concentration of CTZ
530 decreased (Table 2), suggesting a further oxidation of CTZ by $^{\bullet}$OH and a formation of second
531 generation TPs. This was confirmed by the detection of HCTZ-TP3, -TP4, -TP5 and -TP7 in O_3-EFF
532 in addition to CTZ (data not shown).

4. Conclusions

- Apparent second-order rate constants for the reactions of cetirizine (CTR), fexofenadine (FXF) and hydrochlorothiazide (HCTZ) with ozone at pH 7 are high ($k_{O3,pH7}$ of $1.7 \cdot 10^5$ $M^{-1}s^{-1}$, $9.0 \cdot 10^3$ $M^{-1}s^{-1}$ and $8.5\ 10^4$ $M^{-1}s^{-1}$, for CTR, FXF and HCTZ, respectively) warranting an efficient abatement of these compounds during ozonation of wastewater effluents.
- Ozone TPs were determined and the mechanisms for the formation of 8 TPs of cetirizine and hydrochlorothiazide, respectively, and 7 TPs of fexofenadine, were elucidated.
- *N*-oxides were quantified with high yields as the primary TPs for the tertiary amines of CTR and FXF.
- Chlorothiazide was shown to be the main ozone transformation product of HCTZ, being formed partly by an electron transfer mechanism (18.5%) and mainly an oxygen transfer mechanism (81.5%).
- Ecotoxicological evaluation with bacteria bioluminescence showed only for the ozonation products of cetirizine slightly increased effects compared to the parent compound. However, the effect concentrations are well above environmentally relevant concentrations.
- Investigations of ozonation performed on a full-scale municipal wastewater treatment plant confirmed the high efficiency of the abatement of the three target compounds. Application of the lowest studied ozone dose (2 g O_3 m^{-3}, 0.35 g O_3 g^{-1} DOC) resulted in an elimination of 92%, 86% and 83% for CTR, HCTZ and FXF, respectively, which is in agreement with the observed apparent second-order rate constants at circumneutral pH ($k_{O3,CTR} > k_{O3,HCTZ} > k_{O3,FXF}$). Concomitantly, the formation of the main TPs, CTR-*N*-oxide, FXF-*N*-oxide and CTZ, was observed.

ACKNOWLEDGEMENT

This work was funded by the EU-FP7 project DEMEAU "Demonstration of promising technologies to address emerging pollutants in water and wastewater" (Grant Agreement no. 308339) and the MICROZO project "Fate of organic micropollutants in advanced treatment of wastewater with ozone" (Project code 12.333) financed by SCIEX- Scientific Exchange Programme NMS.CH. Max Schachtler and his team at the WWPT Neugut are acknowledged for their collaboration. The authors thank

Rebekka Teichler, Elisabeth Salhi, Ursula Schönenberger and Birgit Beck from Eawag for technical support, Holger Lutze from the University of Duisburg-Essen for mechanistic discussions and Sereina Gut and Andrea Schifferli from the Swiss Centre for Applied Ecotoxicology Eawag-EPFL for the measurements of luminescence inhibition.

SUPPORTING INFORMATION

Additional information presented in Text S1-S8, Tables S1-S7 and Fig. S1-S32 are shown in the Supplementary Information.

AUTHOR INFORMATION

Christa S. McArdell, phone +4158 765 5483; fax +41 58 765 5028, email: christa.mcardell@eawag.ch,

Urs von Gunten, phone: +4158 765 5270, fax: +41 58 765 5210, email: urs.vongunten@eawag.ch

References

Acero, J.L., Stemmler, K. and von Gunten, U. (2000) Degradation kinetics of atrazine and its degradation products with ozone and OH radicals: A predictive tool for drinking water treatment. Environ. Sci. Technol. 34(4), 591-597.

Al-Qaim, F.F., Abdullah, M.P., Othman, M.R., Latip, J. and Zakaria, Z. (2014) Multi-residue analytical methodology-based liquid chromatography-time-of-flight-mass spectrometry for the analysis of pharmaceutical residues in surface water and effluents from sewage treatment plants and hospitals. J. Chromatogr. A 1345(0), 139-153.

Bahlmann, A., Carvalho, J.J., Weller, M.G., Panne, U. and Schneider, R.J. (2012) Immunoassays as high-throughput tools: Monitoring spatial and temporal variations of carbamazepine, caffeine and cetirizine in surface and wastewaters. Chemosphere 89(11), 1278-1286.

Benner, J., Salhi, E., Ternes, T. and von Gunten, U. (2008) Ozonation of reverse osmosis concentrate: Kinetics and efficiency of beta blocker oxidation. Water Res. 42(12), 3003-3012.

Benner, J. and Ternes, T.A. (2009) Ozonation of metoprolol: Elucidation of oxidation pathways and major oxidation products. Environ. Sci. Technol. 43(14), 5472-5480.

Bourgin, M., Gervais, G., Bichon, E., Antignac, J.P., Monteau, F., Leroy, G., Barritaud, L., Chachignon, M., Ingrand, V., Roche, P. and Le Bizec, B. (2013) Differential chemical profiling to

589 identify zonation by-products of estrone-sulfate and first characterization of estrogenicity in generated
590 drinking water. Water Res. 47(11), 3791-3802.
591 Brigante, M., DellaGreca, M., Previtera, L., Rubino, M. and Temussi, F. (2005) Degradation
592 of hydrochlorothiazide in water. Environ. Chem. Lett. 2(4), 195-198.
593 Bueno, M.J.M., Gomez, M.J., Herrera, S., Hernando, M.D., Agüera, A. and Fernández-Alba,
594 A.R. (2012) Occurrence and persistence of organic emerging contaminants and priority pollutants in
595 five sewage treatment plants of Spain: Two years pilot survey monitoring. Environ. Pollut. 164(0),
596 267-273.
597 Carbajo, J.B., Petre, A.L., Rosal, R., Herrera, S., Letón, P., García-Calvo, E., Fernández-Alba,
598 A.R. and Perdigón-Melón, J.A. (2015) Continuous ozonation treatment of ofloxacin: Transformation
599 products, water matrix effect and aquatic toxicity. J. Hazard. Mater. 292, 34-43.
600 Castiglioni, S., Bagnati, R., Fanelli, R., Pomati, F., Calamari, D. and Zuccato, E. (2006)
601 Removal of Pharmaceuticals in Sewage Treatment Plants in Italy. Environ. Sci. Technol. 40(1), 357-
602 363.
603 Dantas, R.F., Canterino, M., Marotta, R., Sansa, C., Esplugas, S. and Andreozzi, R. (2007)
604 Bezafibrate removal by means of ozonation: Primary intermediates, kinetics, and toxicity assessment.
605 Water Res. 41(12), 2525-2532.
606 Dodd, M. C., Buffle, M. and von Gunten, U. (2006) Oxidation of Antibacterial Molecules by
607 Aqueous Ozone: Moiety-Specific Reaction Kinetics and Application to Ozone-Based Wastewater
608 Treatment. Environ. Sci. Technol. 40(6), 1969-1977.
609 Fernández, C., González-Doncel, M., Pro, J., Carbonell, G. and Tarazona, J.V. (2010)
610 Occurrence of pharmaceutically active compounds in surface waters of the Henares-Jarama-Tajo river
611 system (Madrid, Spain) and a potential risk characterization. Sci. Total Environ. 408(3), 543-551.
612 Fick, J., Soderstrom, H., Lindberg, R.H., Phan, C., Tysklind, M. and Larsson, D.G.J. (2009)
613 Contamination of Surface, Ground, and Drinking Water from Pharmaceutical Production. Environ.
614 Toxicol. Chem. 28(12), 2522-2527.

615 Garoma, T., Umamaheshwar, S.K. and Mumper, A. (2010) Removal of sulfadiazine,
616 sulfamethizole, sulfamethoxazole, and sulfathiazole from aqueous solution by ozonation.
617 Chemosphere 79(8), 814-820.
618 Gerrity, D., Gamage, S., Holady, J.C., Mawhinney, D.B., Quiñones, O., Trenholm, R.A. and
619 Snyder, S.A. (2011) Pilot-scale evaluation of ozone and biological activated carbon for trace organic
620 contaminant mitigation and disinfection. Water Res. 45(5), 2155-2165.
621 Gustafson, A.L., Stedman, D.B., Ball, J., Hillegass, J.M., Flood, A., Zhang, C.X., Panzica-
622 Kelly, J., Cao, J., Coburn, A., Enright, B.P., Tornesi, M.B., Hetheridge, M. and Augustine-Rauch,
623 K.A. (2012) Inter-laboratory assessment of a harmonized zebrafish developmental toxicology assay –
624 Progress report on phase I. Reprod. Toxicol. 33(2), 155-164.
625 Hennig, U.G.G., Chatten, L.G., Moskalyk, R.E. and Ediss, C. (1981) Benzothiadiazine
626 dissociation constants. Part I. Ultraviolet spectrophotometric pKa determinations. Analyst 106(1262),
627 557-564.
628 Hollender, J., Zimmermann, S.G., Koepke, S., Krauss, M., McArdell, C.S., Ort, C., Singer, H.,
629 von Gunten, U. and Siegrist, H. (2009) Elimination of Organic Micropollutants in a Municipal
630 Wastewater Treatment Plant Upgraded with a Full-Scale Post-Ozonation Followed by Sand Filtration.
631 Environ. Sci. Technol. 43(20), 7862-7869.
632 Huber, M.M., Gobel, A., Joss, A., Hermann, N., Loffler, D., Mcardell, C.S., Ried, A., Siegrist,
633 H., Ternes, T.A. and von Gunten, U. (2005) Oxidation of pharmaceuticals during ozonation of
634 municipal wastewater effluents: A pilot study. Environ. Sci. Technol. 39(11), 4290-4299.
635 Hübner, U., Seiwert, B., Reemtsma, T. and Jekel, M. (2014) Ozonation products of
636 carbamazepine and their removal from secondary effluents by soil aquifer treatment – Indications from
637 column experiments. Water Res. 49, 34-43.
638 Hübner, U., von Gunten, U. and Jekel, M. (2015) Evaluation of the persistence of
639 transformation products from ozonation of trace organic compounds – A critical review. Water Res.
640 68, 150-170.

641 Jeon, J., Kurth, D. and Hollender, J. (2013) Biotransformation Pathways of Biocides and
642 Pharmaceuticals in Freshwater Crustaceans Based on Structure Elucidation of Metabolites Using High
643 Resolution Mass Spectrometry. Chem. Res. Toxicol. 26(3), 313-324.
644 Kim, M., Guerra, P., Shah, A., Parsa, M., Alaee, M. and Smyth, S.A. (2014) Removal of
645 pharmaceuticals and personal care products in a membrane bioreactor wastewater treatment plant.
646 Water Sci. Technol. 69(11), 2221-2229.
647 Kosonen, J. and Kronberg, L. (2009) The occurrence of antihistamines in sewage waters and
648 in recipient rivers. Environ. Sci. Pollut. 16(5), 555-564.
649 Lajeunesse, A., Blais, M., Barbeau, B., Sauvé, S. and Gagnon, C. (2013) Ozone oxidation of
650 antidepressants in wastewater– Treatment evaluation and characterization of new by-products by LC-
651 QToFMS. Chem. Cent. J. 7(15).
652 Lee, Y., Gerrity, D., Lee, M., Encinas Bogeat, A., Salhi, E., Gamage, S., Trenholm, R. A.,
653 Wert, E. C., Snyder, S. A and von Gunten, Urs (2013) Prediction of Micropollutant Elimination during
654 Ozonation of Municipal Wastewater Effluents: Use of Kinetic and Water Specific Information.
655 Environ. Sci. Technol. 47, 5872-5881.
656 Lee, Y., Kovalova, L., McArdell, C. S. and von Gunten, Urs (2014) Prediction of
657 micropollutant elimination during ozonation of a hospital wastewater effluent. Water Res. 64, 134-
658 148.
659 Li, M.-H. (2013) Acute toxicity of 30 pharmaceutically active compounds to freshwater
660 planarians, Dugesia japonica. Toxicol. Environ. Chem. 95(7), 1157-1170.
661 Li, Z., Maier, M.P. and Radke, M. (2014) Screening for pharmaceutical transformation
662 products formed in river sediment by combining ultrahigh performance liquid chromatography/high
663 resolution mass spectrometry with a rapid data-processing method. Anal. Chim. Acta 810, 61-70.
664 Margot, J., Kienle, C., Magnet, A., Weil, M., Rossi, L., de Alencastro, L.F., Abegglen, C.,
665 Thonney, D., Chèvre, N., Schärer, M. and Barry, D.A. (2013) Treatment of micropollutants in
666 municipal wastewater: Ozone or powdered activated carbon? Sci. Total Environ. 461–462, 480-498.
667 Mawhinney, D.B., Vanderford, B.J. and Snyder, S.A. (2012) Transformation of 1H-
668 Benzotriazole by Ozone in Aqueous Solution. Environ. Sci. Technol. 46(13), 7102-7111.

669 McArdell, C. S., Bourgin, M., Teichler, R., Borowska, E., Beck, B., Böhler, M., Fleiner, J.,
670 Salhi, E., von Gunten, U., Hollender, J., Siegrist, H., Kienle, C., Schifferli, A., Ganser, B., Gut, S.,
671 Simon, E., Werner, I., Besselink, H., van der Burg, B. (2015) Demonstration of design, application,
672 controlling and long-term stability of wastewater oxidation, Deliverable D31.1 of EU FP7 project
673 DEMEAU.
674 McDowell, D.C., Huber, M.M., Wagner, M., Von Gunten, U. and Ternes, T.A. (2005)
675 Ozonation of carbamazepine in drinking water: Identification and kinetic study of major oxidation
676 products. Environ. Sci. Technol. 39(20), 8014-8022.
677 Ming, X., Knight, B.M. and Thakker, D.R. (2011) Vectorial Transport of Fexofenadine across
678 Caco-2 Cells: Involvement of Apical Uptake and Basolateral Efflux Transporters. Mol. Pharm. 8(5),
679 1677-1686.
680 Mollica, J.A., Rehm, C.R., Smith, J.B. and Govan, H.K. (1971) Hydrolysis of
681 benzothiadiazines. J. Pharm. Sci. 60(9), 1380-1384.
682 Muñoz, F. and von Sonntag, C. (2000a) Determination of fast ozone reactions in aqueous
683 solution by competition kinetics. J. Chem. Soc. Perk. T. 2 4, 661-664.
684 Muñoz, F. and von Sonntag, C. (2000b) The reactions of ozone with tertiary amines including
685 the complexing agents nitrilotriacetic acid (NTA) and ethylenediaminetetraacetic acid (EDTA) in
686 aqueous solution. J. Chem. Soc. Perk. T. 2 (10), 2029-2033.
687 Nakada, N., Shinohara, H., Murata, A., Kiri, K., Managaki, S., Sato, N. and Takada, H. (2007)
688 Removal of selected pharmaceuticals and personal care products (PPCPs) and endocrine-disrupting
689 chemicals (EDCs) during sand filtration and ozonation at a municipal sewage treatment plant. Water
690 Res. 41(19), 4373-4382.
691 Nödler, K., Voutsa, D. and Licha, T. (2014) Polar organic micropollutants in the coastal
692 environment of different marine systems. Marine Pollut. Bull. 85(1), 50-59.
693 Nöthe, T., Fahlenkamp, H. and Sonntag, C.v. (2009) Ozonation of Wastewater: Rate of Ozone
694 Consumption and Hydroxyl Radical Yield. Environ. Sci. Technol. 43(15), 5990-5995.

695 Oosterhuis, M., Sacher, F. and ter Laak, T.L. (2013) Prediction of concentration levels of
696 metformin and other high consumption pharmaceuticals in wastewater and regional surface water
697 based on sales data. Sci. Total Environ. 442, 380-388.
698 Pryor, W. A., Giamalva, D. H. and Church D. F. (1984) Kinetics of ozonation. 2. Amino acids
699 and model compounds in water and comparison to rates in nonpolar solvents. J. Am. Chem. Soc. 106,
700 7094–7100.
701 Real, F.J., Acero, J.L., Benitez, F.J., Roldán, G. and Fernández, L.C. (2010) Oxidation of
702 hydrochlorothiazide by UV radiation, hydroxyl radicals and ozone: Kinetics and elimination from
703 water systems. Chem. Eng. J. 160(1), 72-78.
704 Sanderson, H., Johnson, D.J., Reitsma, T., Brain, R.A., Wilson, C.J. and Solomon, K.R.
705 (2004) Ranking and prioritization of environmental risks of pharmaceuticals in surface waters.
706 Regulat. Toxicol. Pharma. 39(2), 158-183.
707 Schymanski, E.L., Jeon, J., Gulde, R., Fenner, K., Ruff, M., Singer, H.P., Hollender, J. (2014)
708 Identifying Small Molecules via High Resolution Mass Spectrometry: Communicating Confidence.
709 Environ. Sci. Technol. 48(4), 2097-2098.
710 Tam, K.Y. and Quere, L. (2001) Multiwavelength spectrophotometric resolution of the micro-
711 equilibria of cetirizine. Anal. Sci. 17(10), 1203-1208.
712 Vaghela, B., Rao, S.S., Reddy, A.M., Venkatesh, P. and Kumar, N. (2012) Identification and
713 Characterization of an Oxidative Degradation Product of Fexofenadine, Development and Validation
714 of a Stability-Indicating RP-UPLC Method for the Estimation of Process Related Impurities and
715 Degradation Products of Fexofenadine in Pharmaceutical Formulations. Sci. Pharm. 80(2), 295-309.
716 von Sonntag, C. and von Gunten, U. (2012) Chemistry of ozone in water and wastewater
717 treatment, IWA Publishing, London.
718 Vujić, Z., Mulavdić, N., Smajić, M., Brborić, J. and Stankovic, P. (2012) Simultaneous
719 Analysis of Irbesartan and Hydrochlorothiazide: An Improved HPLC Method with the Aid of a
720 Chemometric Protocol. Molecules 17(3), 3461.

721 Webb, S.F. (2001) A data-based perspective on the environmental risk assessment of human
722 pharmaceuticals I - Collation of available ecotoxicity data. Pharmaceuticals in the Environment, 175-
723 201.
724 Yao, D.C.C. and Haag, W.R. (1991) Rate constants for direct reactions of ozone with several
725 drinking water contaminants. Water Res. 25(7), 761-773.
726 Yasui-Furukori, N., Uno, T., Sugawara, K. and Tateishi, T. (2005) Different effects of three
727 transporting inhibitors, verapamil, cimetidine, and probenecid, on fexofenadine pharmacokinetics.
728 Clin. Pharmacol. Ther. 77(1), 17-23.
729 Zimmermann, S.G., Schmukat, A., Schulz, M., Benner, J., von Gunten, U. and Ternes, T.A.
730 (2012) Kinetic and mechanistic investigations of the oxidation of tramadol by ferrate and ozone.
731 Environ. Sci. Technol. 46(2), 876-884.
732 Zimmermann, S.G., Wittenwiler, M., Hollender, J., Krauss, M., Ort, C., Siegrist, H. and von
733 Gunten, U. (2011) Kinetic assessment and modeling of an ozonation step for full-scale municipal
734 wastewater treatment: Micropollutant oxidation, by-product formation and disinfection. Water Res.
735 45(2), 605-617.
736
737
738

739 Figures captions

740 Fig. 1. pH dependence of the apparent second-order rate constants for the reaction of ozone with (a)
741 cetirizine (CTR), (b) fexofenadine (FXF), (c) hydrochlorothiazide (HCTZ), at T=20 ^{o}C, $[CTR]_0$ =
742 $[FXF]_0$ = $[HCTZ]_0$ = 40 μM. Values of k_{O3} were determined by competition kinetics using the
743 following competitors: (♦) *p*-cresol; (●) *trans*-cinnamic acid; (▲) 1,4-benzoquinone; (■) orotic acid.
744 The lines correspond to the calculated pH-dependence of the apparent second-order rate constants (see
745 Table 1) using for (i) cetirizine, pK_{a1}=2.1, pK_{a3}=7.0, (ii) fexofenadine, pK_{a2}=9.0, (iii)
746 hydrochlorothiazide, pK_{a1} = 7.0, pK_{a2} = 10.5.

747 Fig. 2. Ozonation pathways for (a) cetirizine (CTR), (b) fexofenadine (FXF) and (c)
748 hydrochlorothiazide (HCTZ). TPs marked with dashed frames are available as commercial standards,
749 and with hash (#) are formed in very low yields; (pH 7, T=20 ^{0}C, [*t*-BuOH]=100 mM, ozone:target
750 compound molar ratio 0.1-10).

751 Fig. 3. Bench-scale ozonation of hydrochlorothiazide (1.6 μmol in 8 mL) in presence of *t*-BuOH (400
752 mM). Ozone dose (diamond) and formed formaldehyde (square) as a function of the consumed
753 hydrochlorothiazide after complete depletion of ozone. Inset: Formation of chlorothiazide as a
754 function of the consumed hydrochlorothiazide after complete depletion of ozone.

755 Fig. 4. Formation mechanisms of chlorothiazide (HCTZ-TP1) from hydrochlorothiazide (a) through
756 two electron-transfer reactions, (b) via an oxygen transfer pathway.

757 Fig. 5. Abatement of (a) cetirizine (CTR), (b) fexofenadine (FXF) and (c) hydrochlorothiazide
758 (HCTZ) and the formation of the corresponding TPs during ozonation at various ozone:target
759 compound molar ratios of 0.1-10 (pH 7, T=20 ^{0}C, [*t*-BuOH]=100 mM). For all TPs shown commercial
760 standards were available. For evolution of TPs without standards see Figs. S5-S10.

761

762 Tables captions

763 Table 1

764 Species-specific and apparent second-order rate constants for the reaction of ozone with the parent
765 compounds and with selected TPs (T=20 ^{0}C, [*t*-BuOH] =20-100 mM).

766 Table 2

767 Average concentrations (± standard deviation) (ng L^{-1}), % elimination of the target compounds
768 cetirizine, fexofenadine and hydrochlorothiazide and the formation of TPs during full-scale ozonation
769 at WWTP Neugut, Dübendorf, Switzerland (pH 7.4-7.9, T=18.2-22.3 ^{0}C, 0.01 - 0.04 mg NO_2^-N L^{-1},
770 DOC= 4.7-5.7 mg L^{-1}, alkalinity 4-5 mM).

771

Supplementary Information

Oxidation of cetirizine, fexofenadine and hydrochlorothiazide during ozonation: Kinetics and transformation products

Ewa Borowska [1,2], *Marc Bourgin* [1], *Juliane Hollender* [1,3], *Cornelia Kienle*[4], *Christa S. McArdell* [1*], *Urs von Gunten* [1,3,5*]

[1]Eawag, Swiss Federal Institute of Aquatic Science and Technology, CH-8600 Dübendorf, Switzerland

[2]Silesian University of Technology, Faculty of Power and Environmental Engineering, Environmental Biotechnology Department, PL-44100 Gliwice, Poland

[3]Institute of Biogeochemistry and Pollutant Dynamics (IBP), ETH Zurich, CH-8092 Zurich, Switzerland

[4]Swiss Centre for Applied Ecotoxicology Eawag-EPFL, Überlandstrasse 133, CH-8600 Dübendorf, Switzerland

[5]School of Architecture, Civil and Environmental Engineering (ENAC), Ecole Polytechnique Fédérale de Lausanne (EPFL), CH-1015 Lausanne, Switzerland

*CORRESPONDING AUTHORS: Christa S. McArdell, phone +41 58 765 5483; fax +41 58 765 5802, email: christa.mcardell@eawag.ch, Urs von Gunten, phone: +4158 765 5270, fax: +41 58 765 5210, email: urs.vongunten@eawag.ch.

SUBMITTED TO WATER RESEARCH

SI Content

Text S1 Chemicals and reagents used in the study.

Cetirizine dihydrochloride (purity ≥98%) and fexofenadine hydrochloride (purity ≥98%) were obtained from Tokyo Chemical Industry Deutschland GmbH. Hydrochlorothiazide, chlorothiazide, 4-chlorobenzophenone (≥99%), *tert*-butanol (≥99.5%), triethylamine (≥99%), penten-3-one (≥97%, 0.1% BHT as stabilizer), potassium indigotrisulfonate, 1,4-benzoquinone, orotic acid were purchased from Sigma Aldrich. Cetirizine *N*-oxide (pure) and fexofenadine *N*-oxide were provided by LGC Standards. Azacyclonol (pure), norchlorcyclizine (pure), cetirizine-d_8 dihydrochloride (pure), fexofenadine-d_6 (pure) and hydrochlorothiazide-$^{13}C,d_2$ (pure) were purchased from Toronto Research Chemicals. All solvents (methanol (Merck), acetonitrile (Merck), formic acid (Merck), nanopure water (NPW) were analytical grade (≥99%).

Text S2 Preparation of ozone stock solution.

Ozone stock solutions were prepared by continuously bubbling O_3-containing oxygen through NPW that was cooled in an ice bath (Bader and Hoigné 1981). The concentration of the ozone stock solution was monitored using a direct method (measurement of the O_3 stock solution absorbance at 258 nm using an ε=3200 M^{-1} cm^{-1} (von Sonntag and von Gunten 2012)) or an indigo method (quenching ozone with indigo solution and measurement of solution absorbance at 600 nm using ε= 20 000 M^{-1} cm^{-1} (Bader and Hoigné 1981)).

Table S1 Second –order rate constants of competitors used in this study.

Competitor	pK_a	k_{O3} $[M^{-1}s^{-1}]$	Form	Reference
***trans*-Cinnamic acid**	4.4	5×10^4	Molecular	Leitzke et al. 2001
		3.8×10^5	Anionic	Leitzke et al. 2001
***p*-Cresol**	10.2	3×10^4	Molecular	Hoigné and Bader 1983
		1.1×10^9	Anionic	This study[1]
Penten-3-one	-	5.9×10^4	Molecular	Peter and von Gunten 2007
1,4-Benzoquinone	-	2.5×10^3	Molecular	Mvula and von Sonntag 2003
Orotic acid	2.1, 9.5	5.9×10^3	Molecular	Theruvathu et al. 2001

[1] estimated by competition kinetics with *trans*-cinnamic acid at pH 7

Text S3 Determination of second-order rate constant using competition kinetics.

Second order rate constants for the reaction of the selected compounds with ozone were measured using competition kinetics (Muñoz and von Sonntag 2000, Huber et al. 2003). Experiments were performed in a series of 8 ml vials containing 70 µM of target compound and 100 µM of a reference compound (competitor with known ozone reactivity). 20-100 mM *tert*-butanol (*t*-BuOH) was used as a radical scavenger and pH was maintained constant by a 40-50 mM phosphate buffer. Each vial was spiked with the ozone stock solution to reach a concentration in the range of 10-160 µM. The mixtures were stirred on a magnetic stirrer for few seconds to mix ozone in. Samples were withdrawn from the vials when complete ozone depletion was achieved. The residual concentrations of substances (target and reference compounds) were determined by HPLC-DAD (Table S2).
The second-order rate constant was calculated from the Eq. S1

$$-ln\left(\frac{[C]}{[C]_0}\right) = \frac{k_{C,O3}}{k_{R,O3}} \times \left(-ln\left(\frac{[R]}{[R]_0}\right)\right) \quad \text{(S1)}$$

As shown in Eq. S1, there is a linear dependence between the natural logarithm of the relative residual concentration of the target compound (C) and the natural logarithm of the relative residual concentration of the reference compound (R) with the ratio of the corresponding second order rate constants, $k_{C,O3}$ and $k_{R,O3}$, as the slope. Using the known second-order rate constant of the reference compound and the slope of the linear function, the second-order rate constant of the target compound can be calculated.

Considering pH-dependence of the second-order rate constant (see SI Text S5), competitor is selected based on the expected reactivity of the investigated compound, but also based on the experimental conditions (pH).

Results of the kinetic study discussed in the publication are presented in the SI Table S2.

Text S4 Determination of second-order rate constants under pseudo-first order conditions by monitoring of the target compound in excess of ozone.

Due to their very low water solubility and/or expected low reactivity with ozone, the second-order rate constants for reaction of 4-CBP, FXF *N*-oxide and CTZ with ozone were determined under pseudo-first order conditions with excess of ozone (Yao and Haag 1991). The initial concentration of ozone was ≥20-times higher than the initial concentration of the target compound. Experiments were performed in 250-mL bottles equipped with a dispenser system (Hoigné and Bader 1994) at a temperature of 20±2 ºC. The solution was buffered at pH 7 with 50 mM phosphate buffer. To prevent the oxidation by hydroxyl radicals, 100 mM *t*-BuOH were used to quench hydroxyl radicals. An aliquot of the ozone stock solution was injected to the system and the mixture was stirred for 5 seconds to obtain homogenous conditions. Aliquots of the ozonated solution (2 mL) were withdrawn

at fixed time points in duplicate. In the first sample, residual ozone was quenched with a solution of indigo and the sample was used for the determination of dissolved ozone concentration in the system. The concentration of ozone was measured spectrophotometrically using the indigo method (Text S2) and based on these values the ozone exposure ($\int_0^t [O_3]dt$) could be calculated. In the second withdrawn sample, ozone was quenched with sodium sulfite (2 mL, 0.5 mM in Nanopure water) and the sample was used for determination of the residual concentration of the investigated compound by HPLC-DAD.

The apparent second-order rate constant (k_{app}) was calculated based on Eq. S2.

$$-ln\left(\frac{[C]}{[C]_0}\right) = k_{app} \int_0^t [O_3]dt \quad \text{(S2)}$$

By plotting the natural logarithm of the relative residual compound (C) concentration $-ln\left(\frac{[C]}{[C]_0}\right)$ versus the ozone exposure ($\int_0^t [O_3]dt$), a linear function was obtained. The slope of the function corresponds to the apparent second-order rate constant (k_{app}) at the given pH.

Results obtained in the kinetic study are compiled in the Table S2.

Table S2 Results of kinetic studies of CTR, FXF and HCTZ and their TPs.

Compound	pH	Method	$k_{O3,competitor}\ [M^{-1}s^{-1}]$	Slope of linear function	Linearity	$k_{O3}\ [M^{-1}s^{-1}]$
Cetirizine	2	Competition kinetics with *p*-cresol[2]	3.0×10^4	0.20± 0.01	≥0.99	$6.1(\pm 0.3) \times 10^3$
	3		3.0×10^4	0.21±0.01	≥0.99	$6.3(\pm 0.1) \times 10^3$
	4		3.1×10^4	0.17±0.01	≥0.99	$5.2(\pm 0.1) \times 10^3$
	5		3.7×10^4	0.17±0.01	≥0.98	$6.3(\pm 0.1) \times 10^3$
	6		9.7×10^4	0.25±0.02	≥0.98	$2.4(\pm 0.7) \times 10^4$
	6.5		2.4×10^5	0.31±0.01	≥0.98	$7.5(\pm 0.2) \times 10^4$
	7	Competition kinetics with *trans*-cinnamic acid	3.8×10^5	0.45±0.01	≥0.99	$1.7(\pm 0.1) \times 10^5$
	8			0.62±0.01	≥0.99	$2.4(\pm 0.1) \times 10^5$
	9			0.74±0.01	≥0.98	$2.8(\pm 0.1) \times 10^5$
	11			0.94±0.01	≥0.99	$3.4(\pm 0.1) \times 10^5$
Cetirizine *N*-oxide	7	Competition kinetics with penten-3-one	5.9×10^4	0.14±0.01	≥0.99	$8.1(\pm 0.1) \times 10^3$
4-Chlorobenzophenone	7	Monitoring of target compound	n.a.[3]	0.40±0.05	≥0.94	0.40 ± 0.05
Norchlorcyclizine	7	Competition kinetics with penten-3-one	5.9×10^4	0.36±0.01	≥0.97	$2.1(\pm 0.1) \times 10^4$
Fexofenadine	7	Competition kinetics with 1,4-benzoquinone	2.5×10^3	3.56±0.30	≥0.99	$9.0(\pm 0.1) \times 10^3$
	7.5			5.76±0.11	≥0.99	$1.4(\pm 0.1) \times 10^4$
	8	Competition kinetics with *trans*-cinnamic acid	3.8×10^5	0.30±0.01	≥0.99	$1.1(\pm 0.1) \times 10^5$
	8.5			0.49±0.02	≥0.99	$1.9(\pm 0.1) \times 10^5$
	9			0.69±0.01	≥0.99	$2.6(\pm 0.1) \times 10^5$
	9.5			1.13±0.01	≥0.99	$4.3(\pm 0.1) \times 10^5$
	10			1.26±0.01	≥0.99	$4.8(\pm 0.1) \times 10^5$
	11			1.44±0.06	≥0.99	$5.5(\pm 0.2) \times 10^5$
	12			1.50±0.14	≥0.99	$5.7(\pm 0.5) \times 10^5$

[2] *k_{O3} value of p-cresol was calculated at each pH using k_{O3} of its molecular and anionic form (see SI Table S1)*
[3] *n.a. not applicable*

Fexofenadine *N*-oxide	7	Monitoring of target compound	n.a	6.0±2.0	≥0.91	$\sim 6.0 \pm 2.0$
Azacyclonol	7	Competition kinetics with 1,4-benzoquinone	2.5×10^3	0.14±0.01	≥0.99	354 ± 15
Hydrochlorothiazide	2	Competition kinetics with orotic acid	5.9×10^3	9.2 ± 0.1	≥ 0.98	$6.5(\pm 0.1) \times 10^2$
	2.5			11.1 ± 0.2	≥ 0.97	$5.4(\pm 0.1) \times 10^2$
	3			9.4 ± 0.1	≥ 0.98	$6.4(\pm 0.1) \times 10^2$
	3.5			11.5 ± 0.1	≥ 0.96	$5.2(\pm 0.1) \times 10^2$
	4			5.0 ± 0.1	≥ 0.97	$1.2(\pm 0.1) \times 10^3$
	4.5			2.4 ± 0.1	≥ 0.98	$2.5(\pm 0.1) \times 10^3$
	5			1.1 ± 0.1	≥ 0.99	$5.5(\pm 0.1) \times 10^3$
	5.5			0.62 ± 0.01	≥ 0.98	$9.7(\pm 0.1) \times 10^3$
	6	Competition kinetics with *trans*-cinnamic acid	3.7×10^5	26.7 ± 0.1	≥ 0.96	$1.4(\pm 0.1) \times 10^4$
	6.5		3.8×10^5	11.2 ± 0.1	≥ 0.96	$3.4(\pm 0.1) \times 10^4$
	7			4.5 ± 0.1	≥ 0.97	$8.5(\pm 0.1) \times 10^4$
	7.5			2.6 ± 0.1	≥ 0.95	$1.5(\pm 0.1) \times 10^5$
	8			1.4 ± 0.1	≥ 0.86	$2.7(\pm 0.1) \times 10^5$
	8.5			1.3 ± 0.1	≥ 0.96	$3.0(\pm 0.1) \times 10^5$
	9			1.1 ± 0.1	≥ 0.96	$3.4(\pm 0.1) \times 10^5$
	9.5			1.1 ± 0.1	≥ 0.98	$3.5(\pm 0.1) \times 10^5$
	10			0.96 ± 0.01	≥ 0.99	$4.0(\pm 0.1) \times 10^5$
	10.5			0.85 ± 0.01	≥ 0.99	$4.5(\pm 0.1) \times 10^5$
	11			0.75 ± 0.01	≥ 0.99	$5.1(\pm 0.1) \times 10^5$
	11.5			0.73 ± 0.01	≥ 0.98	$5.2(\pm 0.1) \times 10^5$
	12			0.76 ± 0.01	≥ 0.97	$5.0(\pm 0.1) \times 10^5$
	12.5			0.74 ± 0.01	≥ 0.98	$5.1(\pm 0.1) \times 10^5$
Chlorothiazide	7	Monitoring of target compound	n.a.	1.5 ± 0.1	≥ 0.98	1.5 ± 0.1

Text S5 pH-dependence of the apparent second-order rate constant.

The reactivity of the compound with ozone strongly depends on the form in which the compound is present (von Sonntag and von Gunten 2012). In the direct reaction with ozone, the dependence between the apparent second-order rate constant of the reaction of the compound with ozone and the degree of dissociation of the compound can be described as in Equation S3.

$$k_{app} = \alpha k_{BH^+} + (1 - \alpha) k_B \quad \text{(S3)}$$

The observed rate constant (k_{app}) is a sum of rate constant of the protonated (BH^+) and the molecular (B) species of the compounds and the value depends on the degree of dissociation (α) (Hoigné and Bader 1983a). The values k_{BH+} and k_B correspond to species-specific second-order rate constants of protonated and deprotonated form, respectively.

Taking into consideration the pH-dependence of the apparent second-order rate constant and the range of apparent second-order rate constants determined in this study, pK_a values of tertiary amines of FXF and CTR were modeled.

For CTR, the best fit was achieved for a pK_a of 7.0 (Fig. S1a, R^2=0.984), not 8.0 as previously reported (Tam and Quere 2001). The same simulation was performed for FXF and in this case, the highest linearity was achieved for pK_a of 9.0 (Fig. S1b, R^2=0.980), not 9.5 as previously reported (Yasui-Furukori et al. 2005, Ming et al. 2011).

The slope of the regression line (Fig. S1) gives the value of the species-specific rate constant k_{O3} of the molecular forms of substances ($2.8 \cdot 10^5$ M^{-1} s^{-1} for CTR_{MOL} and $5.6 \cdot 10^5$ M^{-1} s^{-1} for FXF_{MOL}).

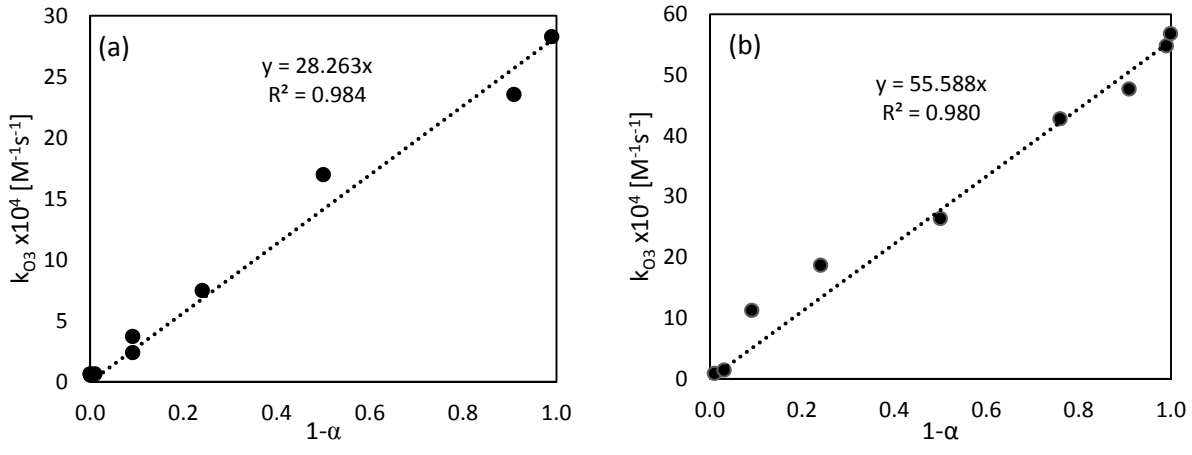

Fig. S1 Plot of k_{O3} for the reaction of (a) cetirizine (pK_{a3}= 7.0), (b) fexofenadine (pK_a=9.0) with ozone versus the degree of dissociation of cetirizine (1-α).

Text S6 Formation of transformation product HCTZ-TP5.

Two differing mechanisms are proposed for the formation of HCTZ-TP5 in Fig. S2. The first one describes the formation of a phenolic intermediate (by the loss of $^1O_2$). This intermediate was not found in ozonated samples, because of the high reactivity of phenol with ozone compared to benzene. The apparent second-order rate constants at pH7 for phenol is $1.4 \cdot 10^6$ M^{-1} s^{-1} (Hoigné and Bader 1983a) while it is 2 M^{-1} s^{-1} for benzene (Hoigné and Bader 1983b).

The second mechanism describes the formation of an ozone adduct and then the loss of an hydroperoxyl radical which reacts immediately in a cage with the molecule to give an organic hydroperoxide and later the 1,4-benzoquinone intermediate HCTZ-TP5 by loss of water (Mvula et al. 2009).

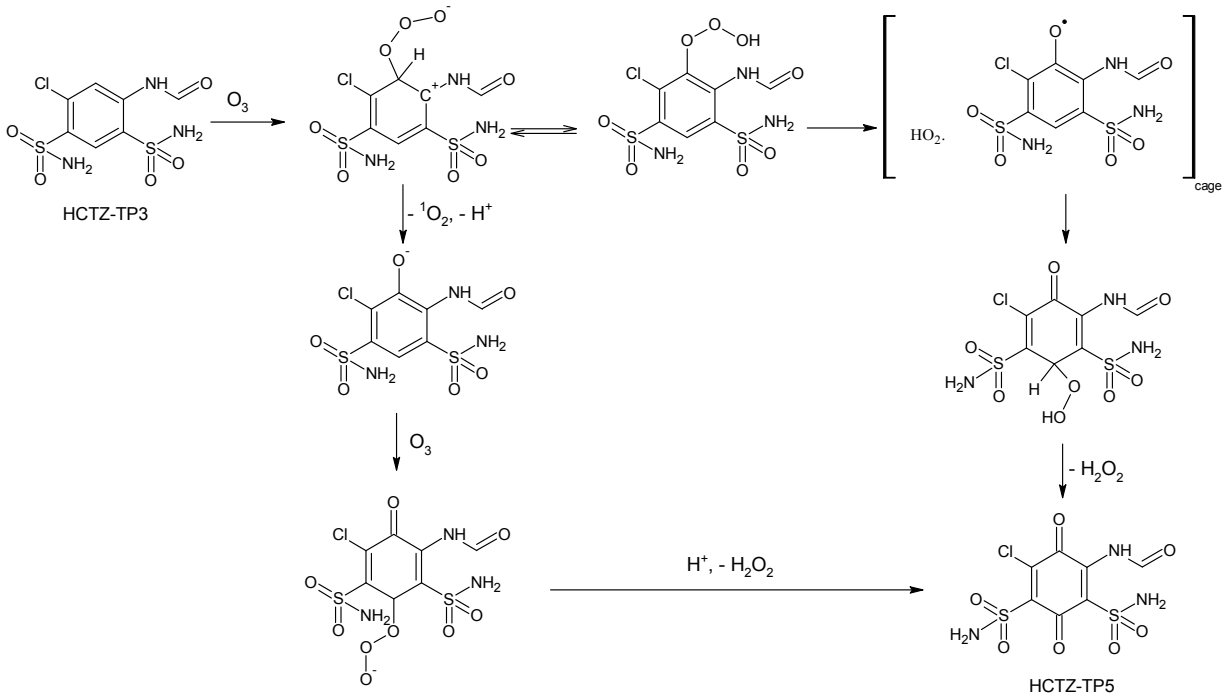

Fig. S2 Proposition of formation mechanisms for the 1,4-benzoquinone derivative (HCTZ-TP5) from the ozonation of HCTZ-TP3.

Text S7 Determination of ecotoxicological effects by a bacteria bioluminescence inhibition assay

The bioluminescence inhibition test is performed with the gram-negative marine bacterium *Aliivibrio fischeri*. Luminescence in this bacterium is coupled directly to the metabolic condition of the cell. Substances that interfere with the cellular energy metabolism cause a decrease in light emission, which is indicative of general toxicity. To evaluate this non-specific toxicity, the level of bioluminescence is measured before bacteria are exposed to a sample and after 30 min of exposure to a sample (Escher et al., 2008, ISO 2007).

The assay was performed on 96-well plates with 3,5-dichlorophenol (3,5-DCP) as a positive control and assay buffer as a negative control (Escher et al. 2008). 3,5-Dichlorophenol was tested in triplicate in a seven-step 2-fold dilution series starting at 3 x 10^{-4} M in the first well; eight replicates were used for negative controls. The spiked water samples were tested in triplicate and in 2-fold dilution series. The lowest dilution factor that could be tested was 2.2. This high sample load was possible by mixing nine parts of an aqueous sample with one part of 10 times concentrated assay buffer. Of this mix, 120 µL were added to a 96-well plate and a 2-fold dilution series was made using one time concentrated assay buffer. Finally, 100 µL were transferred from all wells to 100 µL of a bacteria solution. Samples were tested in the bioluminescence inhibition assay the day after the spiking had been performed.

To calculate the inhibition of bioluminescence, plates containing 100 µL of the bacteria culture per well were measured in a luminescence plate reader shortly before bacteria were exposed to the samples and 30 min after 100 µL of the samples had been added. Bioluminescence values of samples ($I_{samples}$) and controls ($I_{control}$) were entered in Eq. S4.

$$\text{Inhibition [\%]} = \left(1 - \frac{I_{sample}}{I_{control\ (corrected)}}\right) \cdot 100\% \quad \text{(S4)}$$

Bioluminescence inhibition data were then fitted with Eq. S5 to determine EC_{50} and EC_{10} values.

$$\text{Inhibition [\%]} = \frac{100\%}{1 + 10^{\,(log(EC50) - log(concentration)) \cdot slope}} \quad \text{(S5)}$$

Results of the test are depicted in the Fig. S3

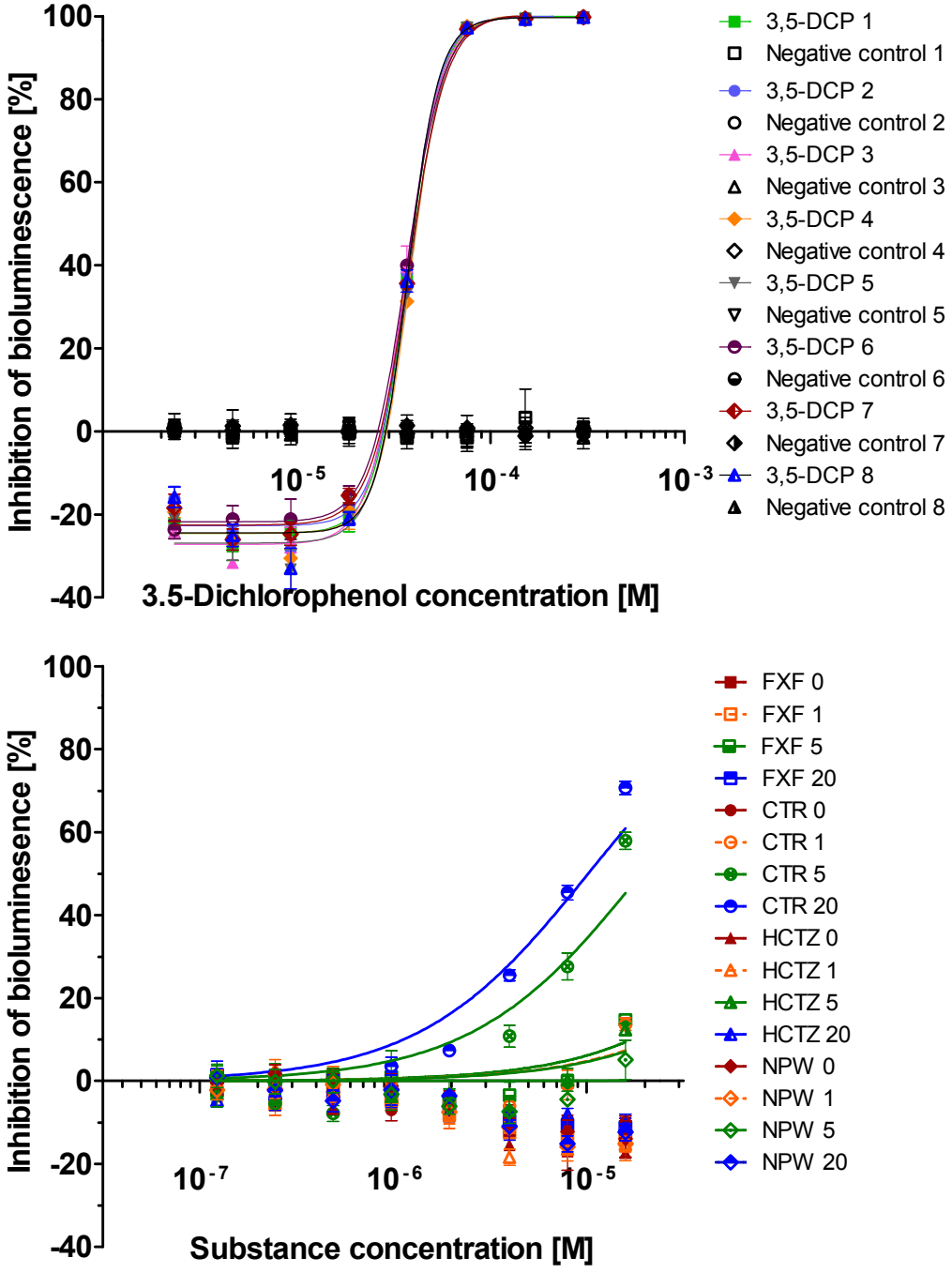

Fig. S3 Inhibition of bioluminescence in bacteria exposed to the reference substance 3.5-dichlorophenol and the negative control (a) and the samples (b). For reference substance and negative control, 1-8 indicate replicate dose-response curves performed on separate 96 well plates. 0, 1, 5, 20 refers to the ozone:compound ratio used in the sample (31-38 µM initial concentration of parent compound).

Table S3 Analytical conditions to determine the target compounds during kinetic experiments - HPLC-DAD.

Cetirizine Cetirizine *N*-oxide 4-Chlorobenzophenone Norchlorcyclizine	Eluent A 0.1% Formic acid in NPW Eluent B Acetonitrile Flow: 500 µL min^{-1} Injection volume: 50 µL Detection: 200 nm	
Time [min]	A [%]	B [%]
0.0	88	12
11.0	88	12
23.0	20	80
23.1	5	95
25.0	5	95
25.1	88	12
30.0	88	12
Fexofenadine Fexofenadine *N*-oxide Azacyclonol	Eluent A 0.05% Triethylamine in NPW, adjusted to pH 7 by 1 M H_3PO_4 Eluent B Acetonitrile Flow: 500 µL min^{-1} Injection volume: 50 µL Detection: 200 nm	
Time [min]	A [%]	B [%]
0.0	75	25
10.0	75	25
15.0	65	35
23.0	40	60
25.0	20	80
26.0	75	25
30.0	75	25
Hydrochlorothiazide Chlorothiazide	Eluent A 0.1% Formic acid in NPW Eluent B Acetonitrile Flow: 600 µL min^{-1} Injection volume: 50 µL Detection: 310 nm	
Time [min]	A [%]	B [%]
0.0	88	12
7.0	88	12
11.0	5	95
12.5	5	95
12.6	88	12
17.0	88	12

Table S4 Analytical conditions to detect the transformation products by LC- HR MS/MS.

Cetirizine Fexofenadine Hydrochlorothiazide	Eluent A 0.1% Formic acid in NPW Eluent B 0.1 % Formic acid in Methanol Flow 300 µL min^{-1} Injection volume: 20 µL	
Time [min]	A [%]	B [%]
0.0	90	10
8.5	50	50
17.0	5	95
25.0	5	95
25.1	90	10
29.0	90	10

Table S5 Analytical conditions to quantify TPs by LC-HRMS.

Cetirizine Fexofenadine Hydrochlorothiazide	Eluent A 0.1% Formic acid in NPW Eluent B 0.1 % Formic acid in Methanol Flow 300 µL min^{-1} Injection volume: 20 µL	
Time [min]	A [%]	B [%]
0.0	95	5
1.5	95	5
17.5	5	95
25.0	5	95
25.1	95	5
29.5	95	50

Table S6 Analytical conditions to quantify HCTZ and chlorothiazide (HCTZ-TP1) by HPLC-DAD.

Hydrochlorothiazide Chlorothiazide	Eluent A 0.1% Formic acid in NPW Eluent B Acetonitrile Flow: 600 µL min^{-1} Injection volume: 50 µL Detection: 310 nm	
Time [min]	A [%]	B [%]
0.0	96	4
5.0	96	4
6.0	88	12
12.0	88	12
12.1	5	95
14.0	5	95
14.1	96	4
19.0	96	4

Text S8 Confirmation of the structure using labeled compounds.

To confirm the structure of TPs, ozonated samples of labeled and non-labeled parent compounds were compared. Based on *m/z* shifts in labeled samples corresponding to deuterium atoms (for HCTZ also ^{13}C atom) in moieties crucial for ozone transformation, the proposed structure of the TPs could be confirmed.

In experiments for identification of CTR TPs, cetirizine-d_8 (CTR-d_8) was used (Fig. S4a), where all 8 hydrogens in the heterocycle are substituted by deuterium atoms.

In the ozonated samples of CTR-d_8, CTR-TP1 had a m/z signal shift of 8.0509 Da compared to the non-labeled CTR, corresponding to the 8 substituted deuterium atoms. This points towards an intact CTR heterocycle in CTR-TP1. The same mass shift of 8.0509 Da was observed for CTR-TP3-8 in ozonated samples of CTR-d_8 in comparison to non-labeled CTR-TPs which also suggest an intact CTR heterocycle. CTR-TP2 had the same *m/z* value in the ozonated samples of CTR-d_8 and non-labeled CTR, which confirmed that CTR-TP2 does not contain the heterocycle.

Hydrochlorothiazide used for ozonation experiments was labeled on the methylene bridge with one ^{13}C and two deuterium (HCTZ-$^{13}C,d_2$, Fig. S4c) atoms between the aniline moiety and sulfonamide group (S^1).

HCTZ-TP1-6 found in the ozonated samples of non-labeled HCTZ had their equivalents in the ozonated samples of labeled HCTZ with a *m/z* shift of 2.01017 corresponding to one ^{13}C and one deuterium, indicating that the site of ozone attack was located at the alkyl group.

For HCTZ-TP7 and HCTZ-TPa/b, the ozonation of the non-labeled and the labeled HCTZ induced the formation of the same compounds as HCTZ-TP7 and HCTZ-TP8a/b, without any mass shift from the isotopes, what confirms that the carbon atom lost during the oxidation is the carbon of the methylene bridge.

A confirmation of the structures by comparison with labeled fexofenadine could not be performed. The only commercially available labeled forms of fexofenadine (FXF-d_6, FXF-d_{10}) contain the deuterium atoms at parts of the molecule which do not react with ozone in a direct reaction (phenyl groups, methyl groups and carboxylic groups).

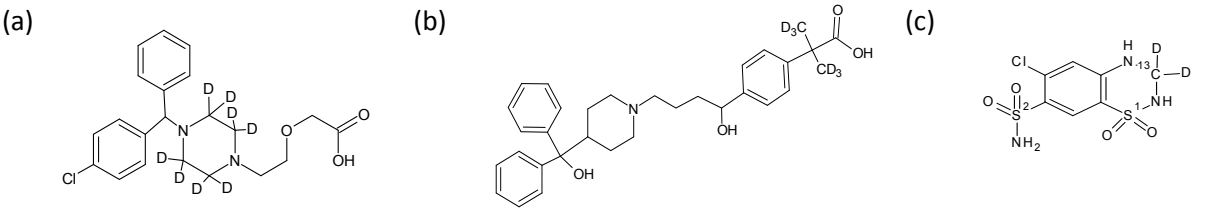

Fig. S4 Labeled compounds used for TPs confirmation in the study: (a) cetirizine-d_8; (b) fexofenadine-d_6; (c) hydrochlorothiazide-$^{13}C,d_2$.

Table S7 LC-MS/MS parameters for cetirizine, fexofenadine and hydrochlorothiazide and their TPs formed during direct reaction with ozone.

Name	RT (min)	Ionization mode	Measured m/z (u)	Accuracy (Δmmu)	Molecular formula	Shift from ozonated labelled compound[4]	Level of confidence (according to Schymanski et al., 2014)
CTR	**17.5**	**ESI(+)**	**389.1627**	**0.283**	**$C_{21}H_{25}O_3N_2Cl$**	**+ 8 d**	**Level 1**
CTR-TP1	17.7	ESI(+)	405.1573	-0.211	$C_{21}H_{25}O_4N_2Cl$	+ 8 d	Level 1
CTR-TP2	20.7	ESI(+)	217.0416	-0.099	$C_{13}H_9OCl$	-	Level 1
CTR-TP3	17.5	ESI(+)	189.1232	-0.319	$C_8H_{16}O_3N_2$	+ 8 d	Level 2b
CTR-TP4	16.8	ESI(+)	287.1309	0.312	$C_{17}H_{19}N_2Cl$	-	Level 1
CTR-TP5	16.3	ESI(+)	421.1523	0.496	$C_{21}H_{25}O_5N_2Cl$	+ 8 d	Level 2b
CTR-TP6/7	17.7	ESI(+)	205.1183	0.284	$C_8H_{16}O_4N_2$	+ 8 d	Level 3
CTR-TP8	16.3	ESI(+)	221.1132	0.358	$C_8H_{16}O_5N_2$	+ 8 d	Level 2b
FXF	**16.0**	**ESI(+)**	**502.2949**	**-0.535**	**$C_{32}H_{39}O_4N$**	**n.a.[5]**	**Level 1**
FXF-TP1	16.1	ESI(+)	518.2901	-0.920	$C_{32}H_{39}O_5N$	n.a.	Level 1
FXF-TP2	14.4	ESI(+)	268.1695	-0.401	$C_{18}H_{21}ON$	n.a.	Level 1
FXF-TP3	11.6	ESI(+)	252.1595	-0.180	$C_{14}H_{21}NO_3$	n.a.	Level 3
FXF-TP4	16.7	ESI(+)	516.2741	-0.830	$C_{32}H_{37}O_5N$	n.a.	Level 3
FXF-TP5/6	14.7	ESI(+)	284.1648	-0.415	$C_{18}H_{21}O_2N$	n.a.	Level 3
FXF-TP7	18.8	ESI(+)	268.1547	-0.035	$C_{14}H_{21}O_4N$	n.a.	Level 3
HCTZ	**9.1**	**ESI(-)**	**295.9572**	**0.012**	**$C_7H_8O_4N_3S_2Cl$**	**+ ^{13}C, + 2 d**	**Level 1**
HCTZ-TP1	9.0	ESI(-)	293.9418	0.013	$C_7H_6O_4N_3S_2Cl$	+ ^{13}C, + d	Level 1
HCTZ-TP2	5.8	ESI(-)	294.9256	0.011	$C_7H_5O_5N_2S_2Cl$	+ ^{13}C, + d	Level 2b
HCTZ-TP3	10.3	ESI(-)	311.9522	0.012	$C_7H_8O_5N_3S_2Cl$	+ ^{13}C, + d	Level 2b
HCTZ-TP4	9.8	ESI(-)	312.9363	0.013	$C_7H_7O_6N_2S_2Cl$	+ ^{13}C, + d	Level 3
HCTZ-TP5	12.2	ESI(-)	341.9258	0.006	$C_7H_6O_7N_3S_2Cl$	+ ^{13}C, + d	Level 3
HCTZ-TP6	12.0	ESI(-)	342.9098	0.006	$C_7H_5O_8N_2S_2Cl$	+ ^{13}C, + d	Level 3
HCTZ-TP7	11.5	ESI(-)	313.9316	0.013	$C_6H_6O_6N_3S_2Cl$	-	Level 3
HCTZ-TP8a/b	9.7/10.7	ESI(-)	314.9153	0.013	$C_6H_5O_7N_2S_2Cl$	-	Level 3

[4] *CTR-d_8; HCTZ-$^{13}C,d_2$*

[5] *n.a.: not applicable*

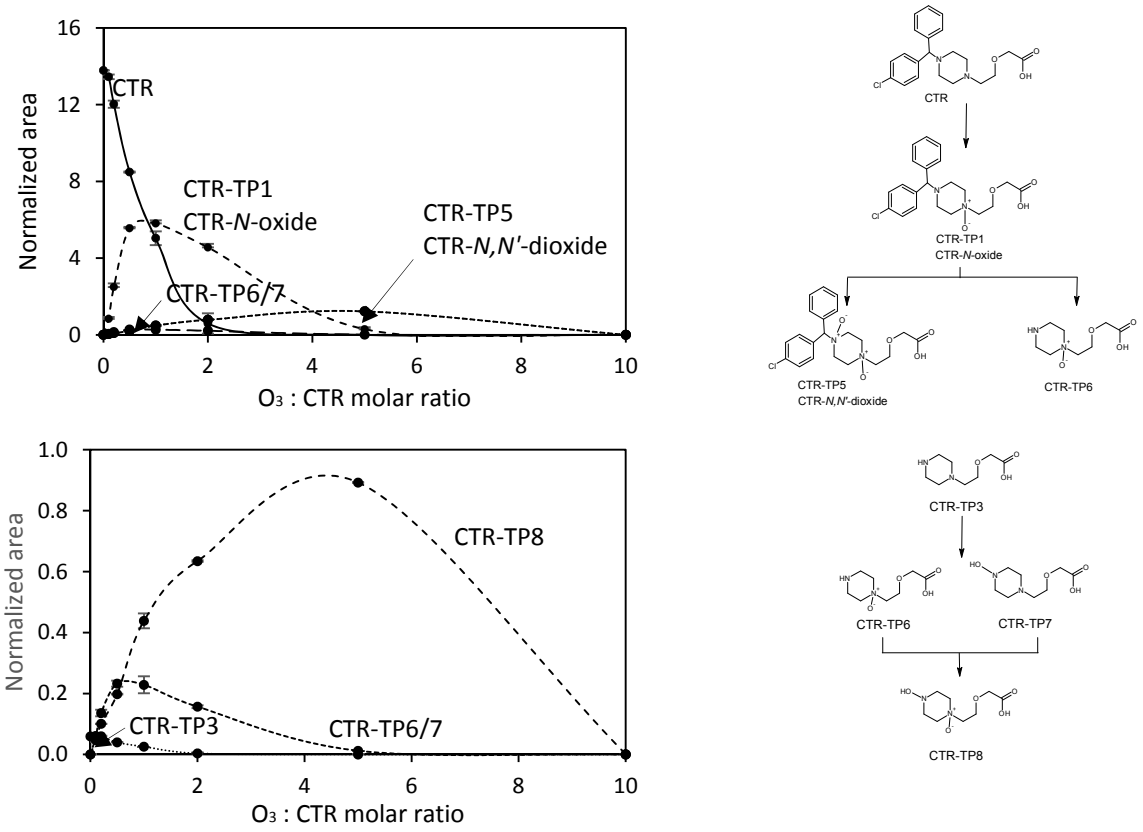

Fig. S5 Semi-quantitative determination of CTR TPs formed during direct reaction of CTR with ozone (pH 7, T=20 ^{0}C, [*t*-BuOH]=100 mM, ozone:target compound molar ratio 0.1-10). The normalized area is the peak area of the TP divided by the peak area of CTR-d_8. The quantification of CTR-TP2 and CTR-TP4 is presented in the manuscript in Fig. 3a.

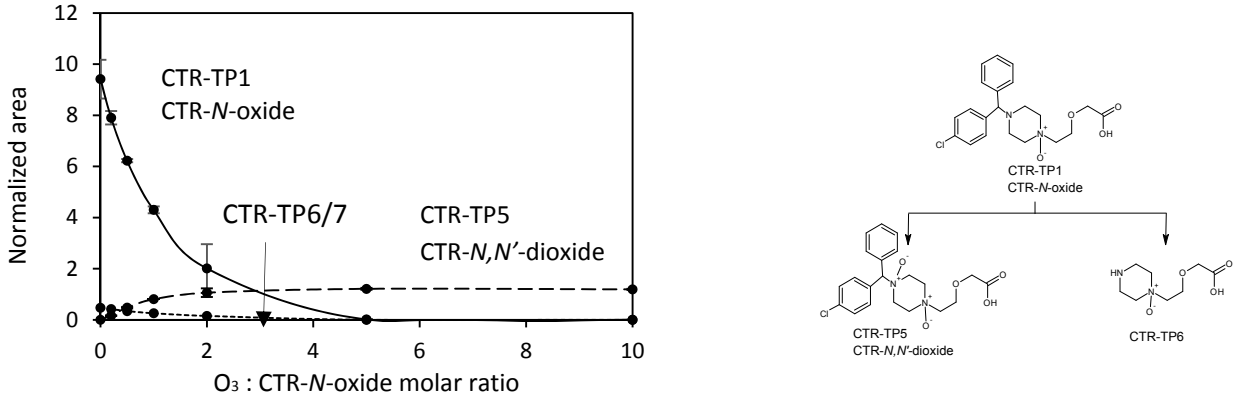

Fig. S6 Semi-quantitative determination of CTR-*N*-oxide TPs formed during direct reaction of CTR-*N*-oxide with ozone (pH 7, T=20 ^{0}C, [*t*-BuOH]=100 mM, ozone:target compound molar ratio 0.1-10). The normalized area is the peak area of the TP divided by the peak area of CTR-d_8.

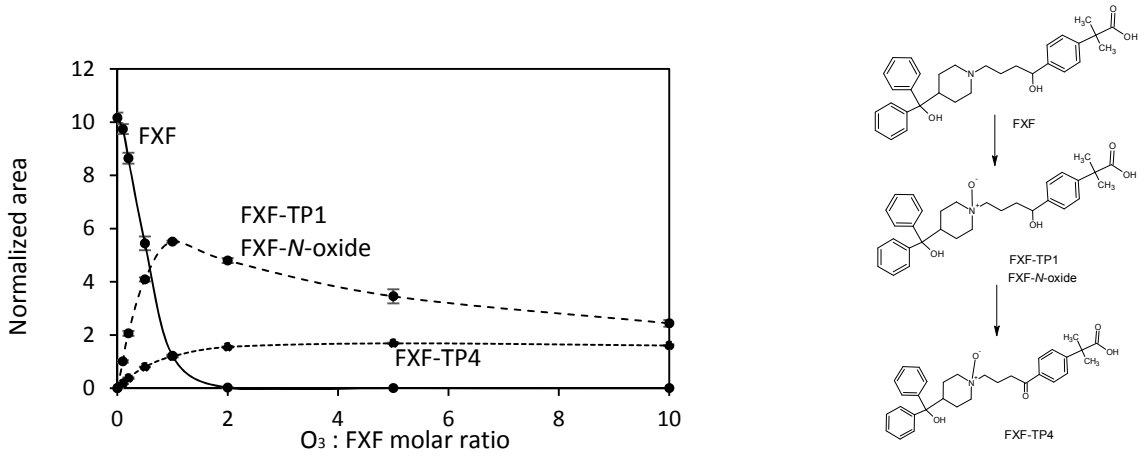

Fig. S7 Semi-quantitative determination of FXF-TPs formed during direct reaction of FXF with ozone (pH 7, T=20 ^{0}C, [*t*-BuOH]=100 mM, ozone:target compound molar ratio 0.1-10). The normalized area is the peak area of the TP divided by the peak area of FXF-d_6. The quantification of FXF-TP2 is presented in the manuscript in Fig. 3b. Data concerning FXF-TP3, -TP5, -TP6 and -TP7 are not shown as signal intensity was very low.

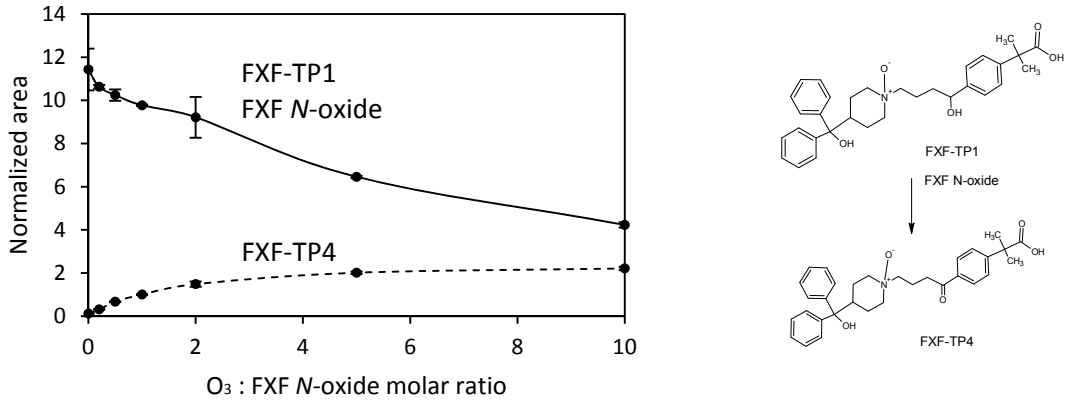

Fig. S8 Semi-quantitative determination of FXF-*N*-oxide TPs formed during direct reaction of FXF-*N*-oxide with ozone (pH 7, T=20 ^{0}C, [*t*-BuOH]=100 mM, ozone:target compound molar ratio 0.1-10). The normalized area is the peak area of the TP divided by the peak area of FXF-d_6.

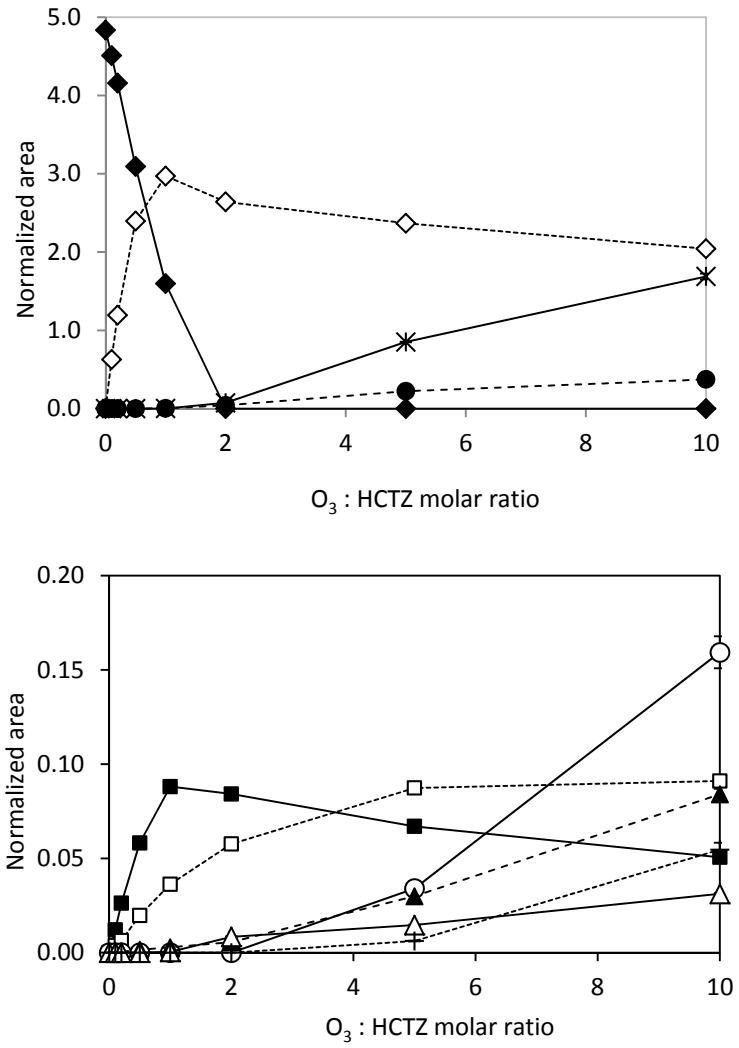

For the structures of HCTZ and HCTZ-TPs see Fig. 2c (main manuscript).

Fig. S9 Semi-quantitative determination of HCTZ and its TPs formed during the reaction of HCTZ with ozone (pH 7, T=20 ^{0}C, [*t*-BuOH]=100 mM, ozone:target compound molar ratio 0.1-10): (♦) HCTZ; (◊) CTZ (HCTZ-TP1); (∗) HCTZ-TP2; (■) HCTZ-TP3; (□) HCTZ-TP4; (●) HCTZ-TP5; (○) HCTZ-TP6; (▲) HCTZ-TP7; (△) HCTZ-TP8a; and (+) HCTZ-TP8b. The normalized area is the peak area of the TP divided by the peak area of HCTZ-d_2,^{13}C.

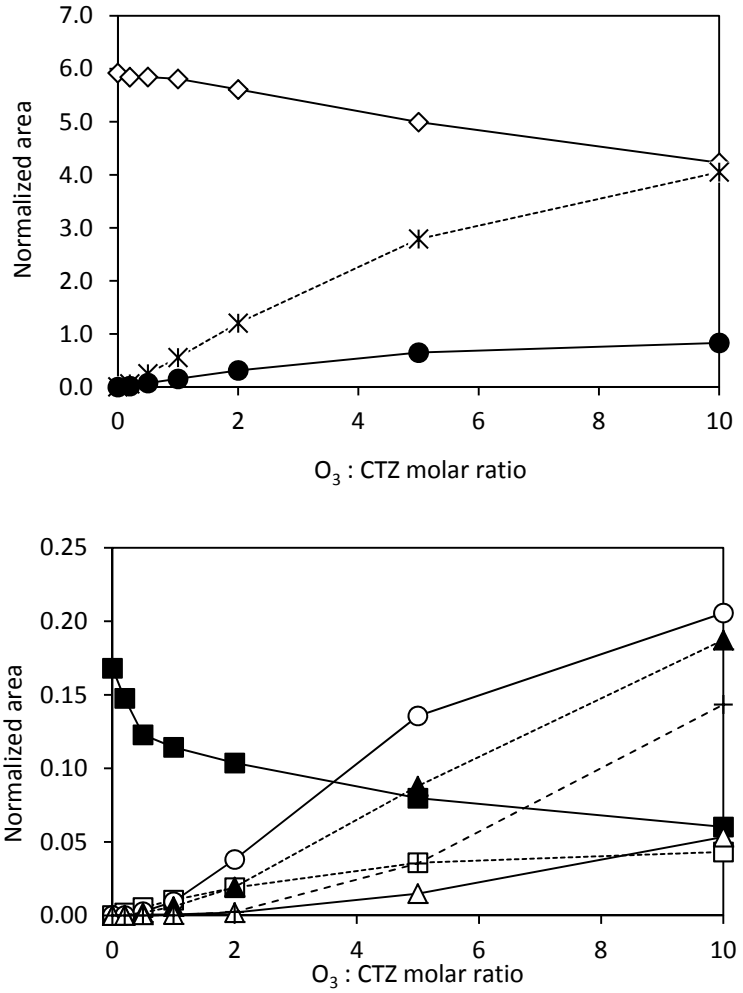

For the structures of CTZ and HCTZ-TPs see Fig. 2c (main manuscript).

Fig. S10 Semi-quantitative determination of CTZ and HCTZ-TPs formed during the reaction of CTZ with ozone (pH 7, T=20 ^{0}C, [*t*-BuOH]=100 mM, ozone:target compound molar ratio 0.1-10): (◊) CTZ (HCTZ-TP1); (✳) HCTZ-TP2; (■) HCTZ-TP3*; (□) HCTZ-TP4; (●) HCTZ-TP5; (○) HCTZ-TP6; (▲) HCTZ-TP7; (△) HCTZ-TP8a; and (+) HCTZ-TP8b. The normalized area is the peak area of the TP divided by the peak area of HCTZ-d_2,^{13}C. *: HCTZ-TP3 was found to be present in the chlorothiazide standard.

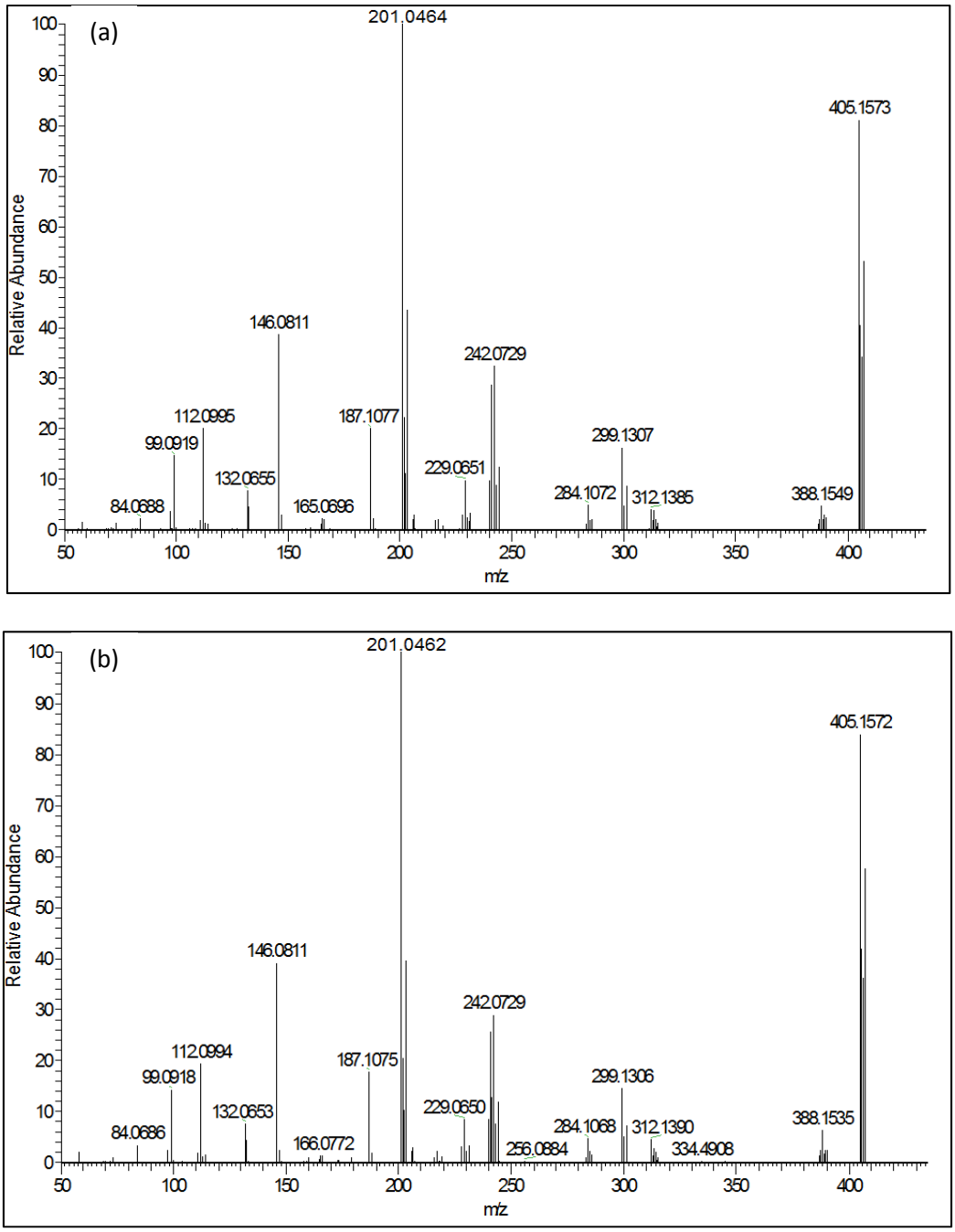

Fig. S11 Comparison of MS^2 spectra of (a) CTR-TP1 with (b) the standard of cetirizine *N*-oxide (FTMS + p ESI Full ms2 405.15 @ hcd 25.00, RT 17.7 min).

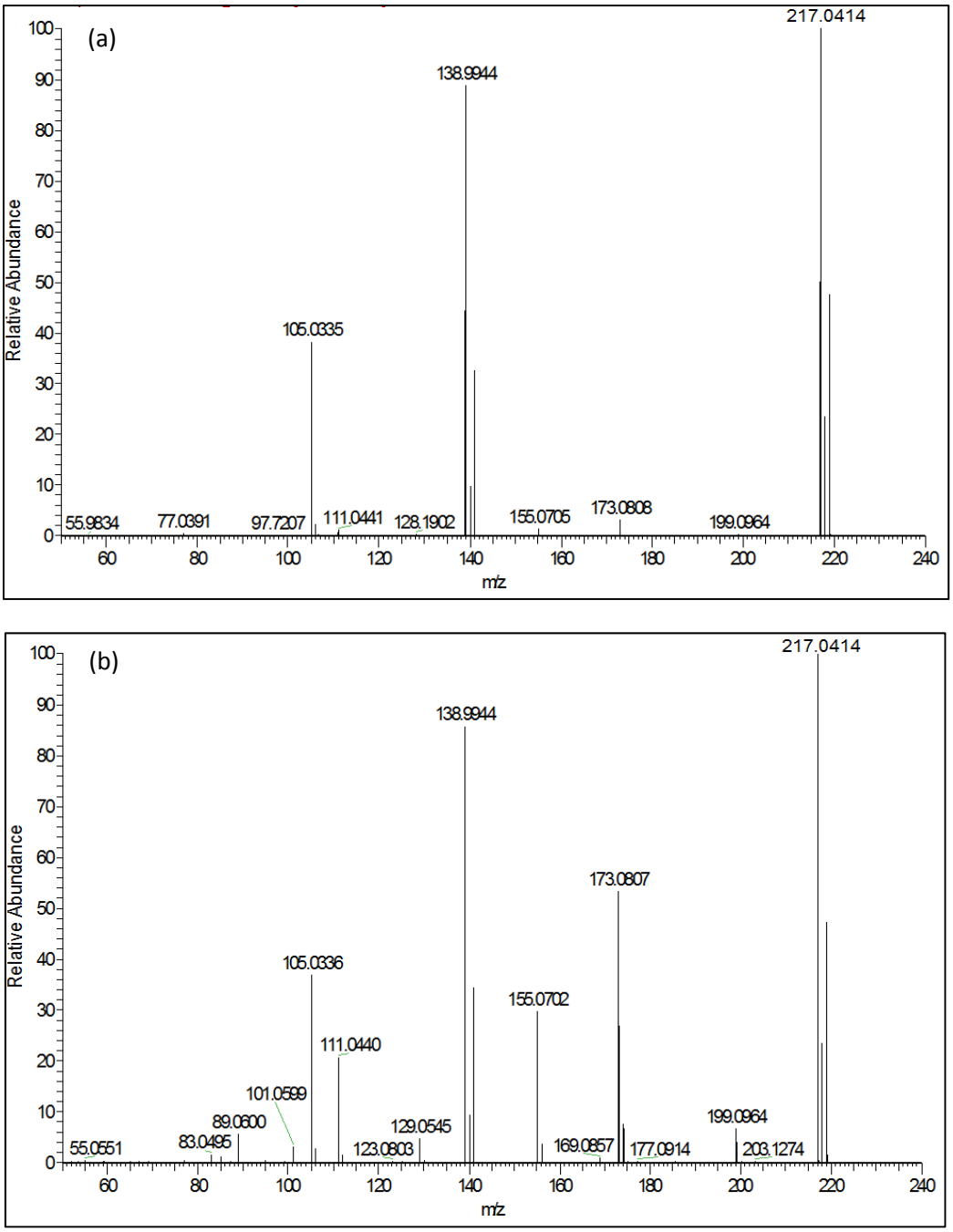

Fig. S12 Comparison of MS^2 spectra of (a) CTR-TP2 with (b) the standard of 4-chlorobenzophenone (FTMS + p ESI Full ms2 217.04 @ hcd 10.00, RT 20.7 min).

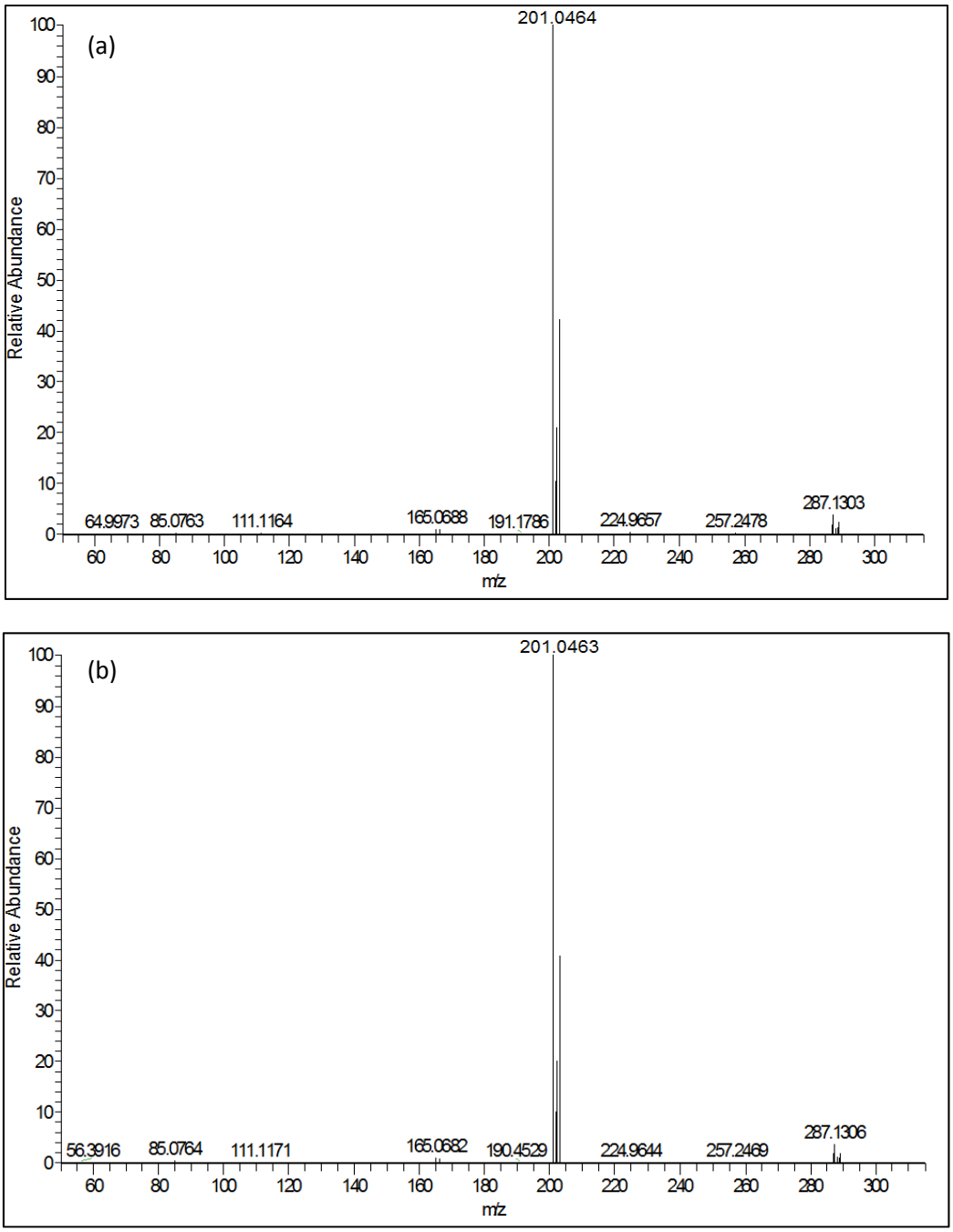

Fig. S13 Comparison of MS^2 spectra of (a) CTR-TP4 with (b) the standard of norchlorocyclizine (FTMS + p ESI Full ms2 287.13 @ hcd 10.00, RT 16.8 min).

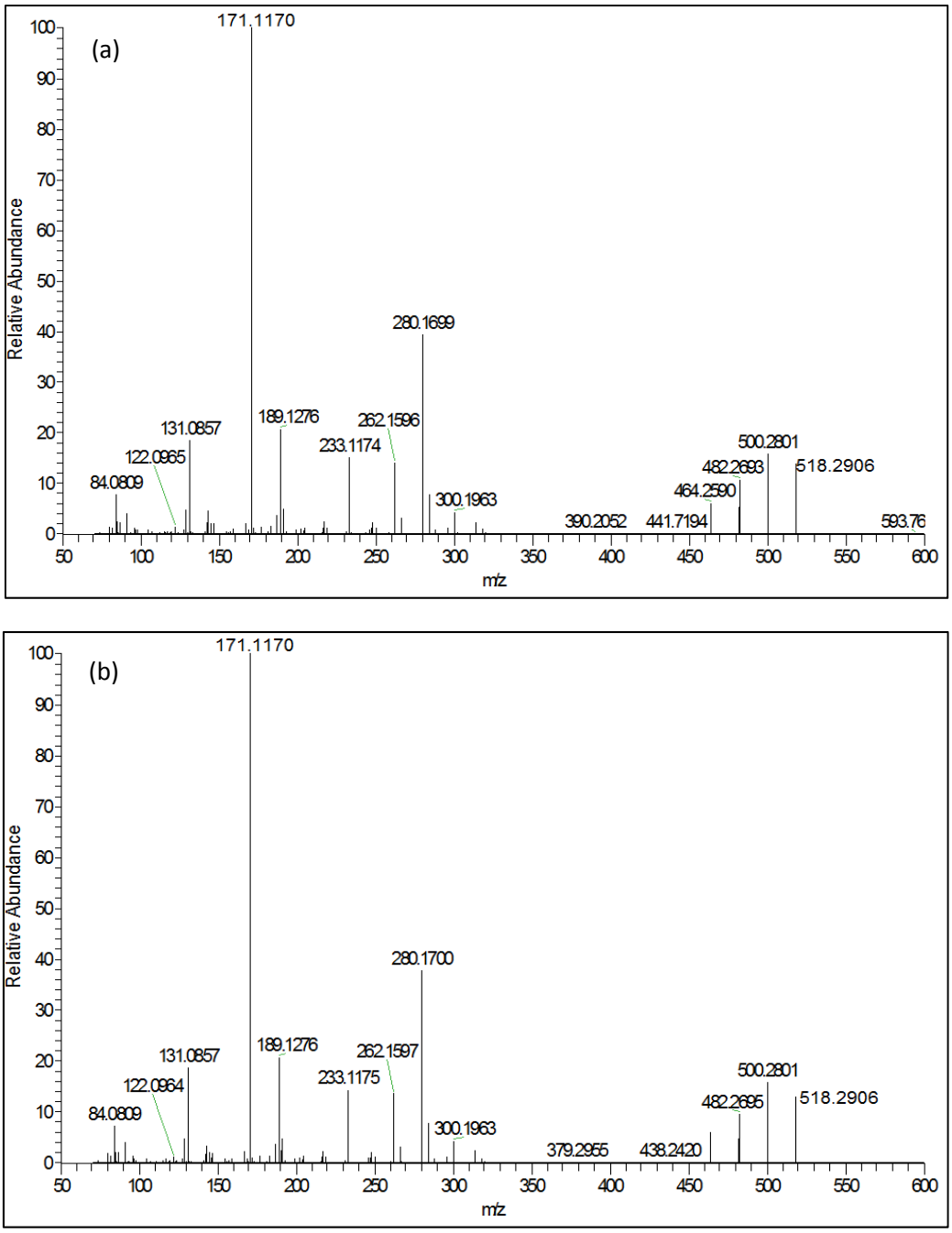

Fig. S14 Comparison of MS^2 spectra of (a) FXF-TP1 with (b) the standard of fexofenadine *N*-oxide (FTMS + p ESI Full ms2 518.29 @ hcd 40.00, RT 16.1 min).

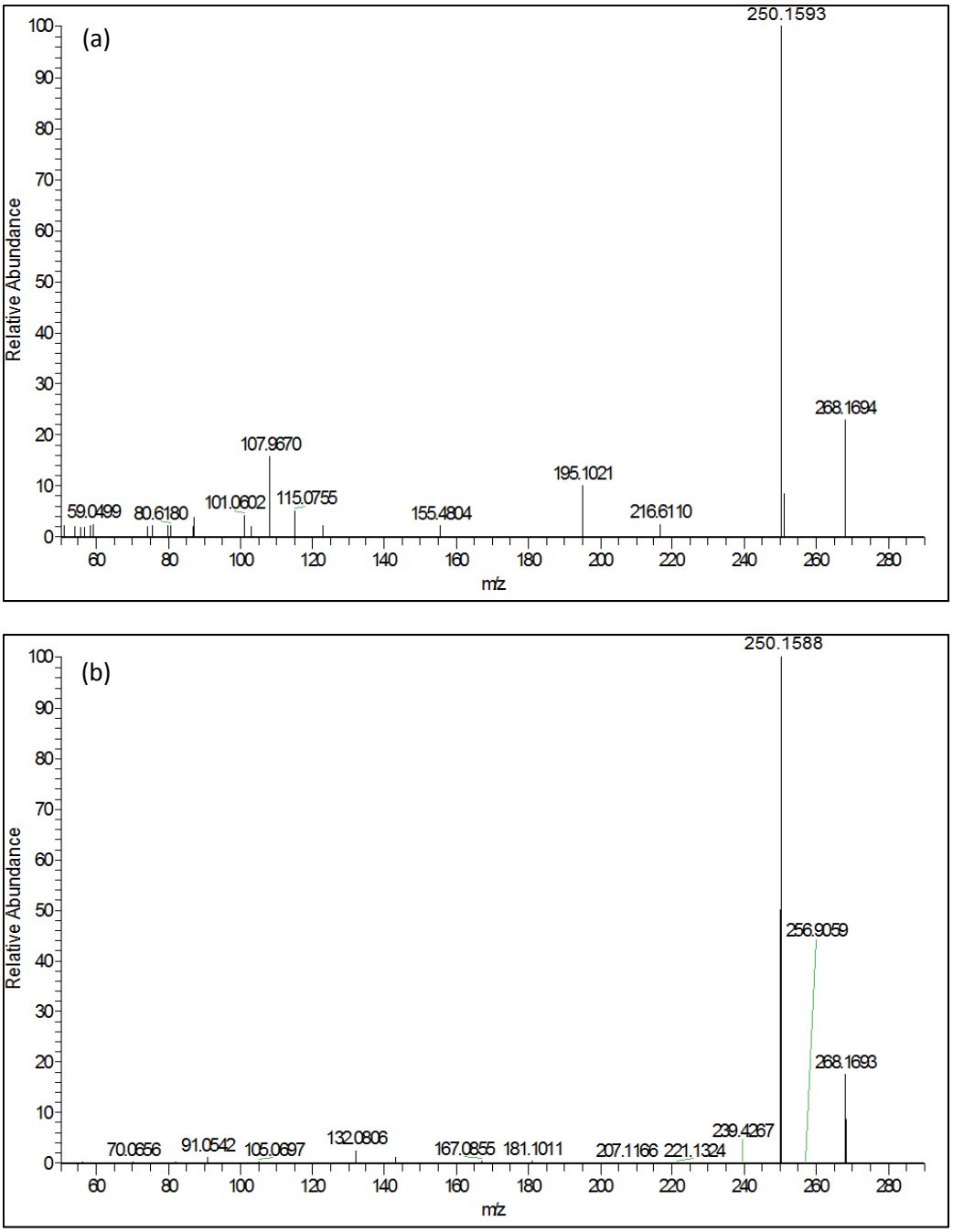

Fig. S15 Comparison of MS^2 spectra of (a) FXF-TP2 with (b) the standard of azacyclonol (FTMS + p ESI Full ms2 268.17 @ hcd 10.00, RT 14.4 min).

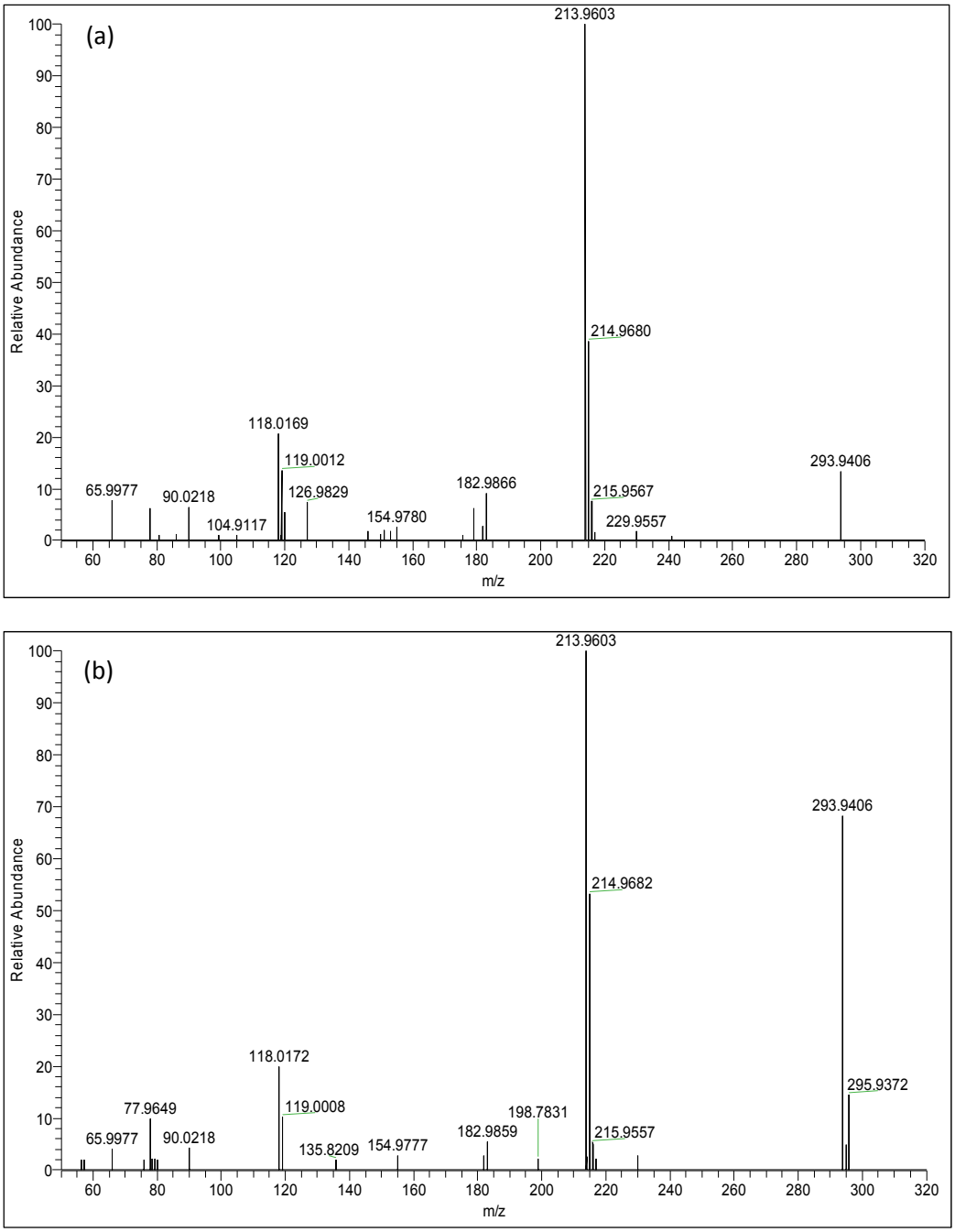

Fig. S16 Comparison of MS^2 spectra of (a) HCTZ-TP1 with (b) the standard of chlorothiazide (FTMS - p ESI Full ms2 293.94 @ hcd 40.00, RT 9.0 min).

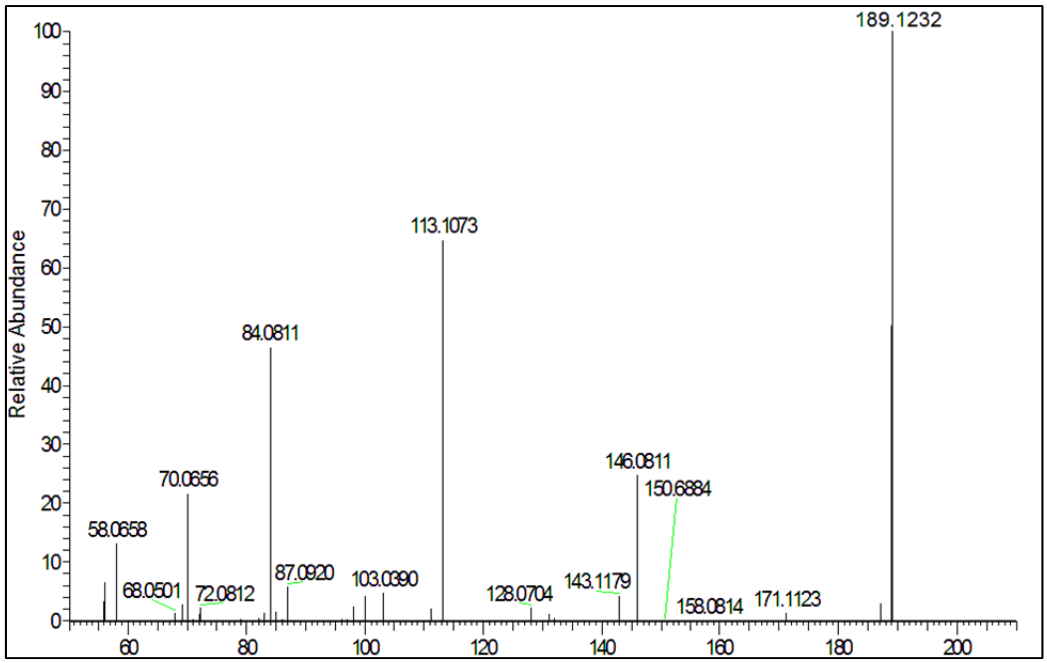

Fig. S17 MS^2 spectrum of CTR-TP3 (FTMS + p ESI Full ms2 189.12 @ hcd 55.00, RT 17.5 min).

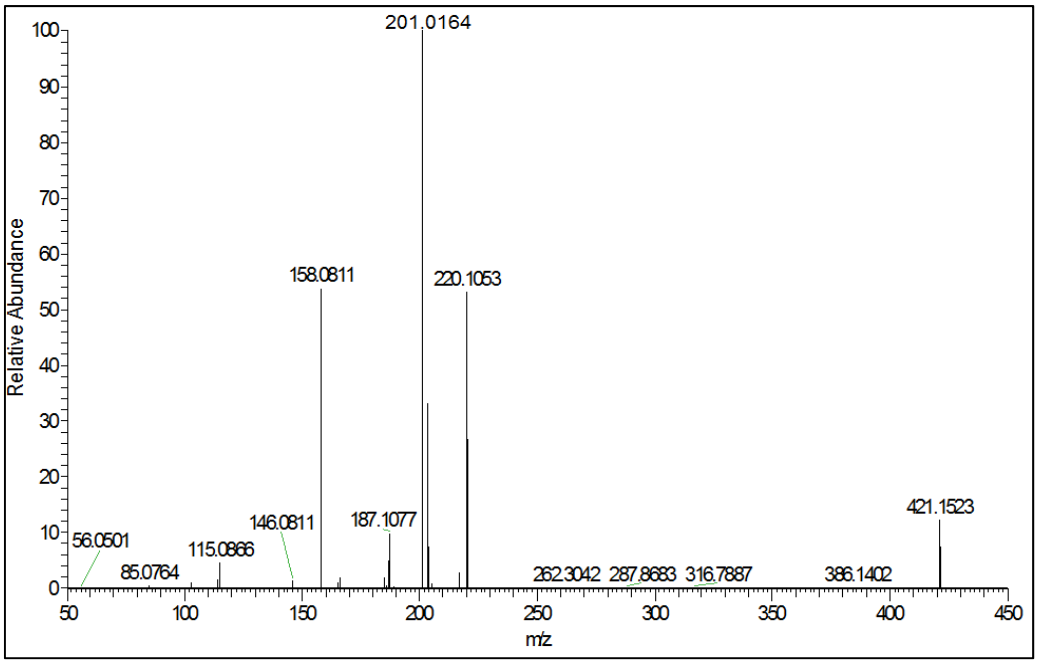

Fig. S18 MS^2 spectrum of CTR-TP5 (FTMS + p ESI Full ms2 421.15 @ hcd 25.00, RT 16.3 min).

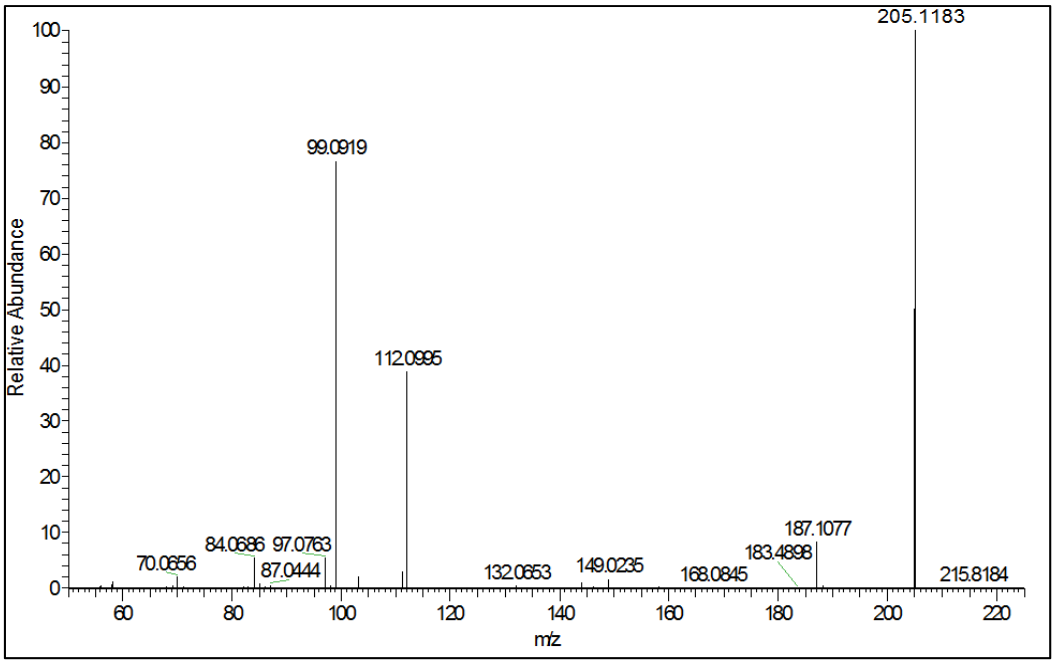

Fig. S19 MS^2 spectrum of CTR-TP6/7 (FTMS + p ESI Full ms2 205.12 @ hcd 40.00, RT 17.7 min.)

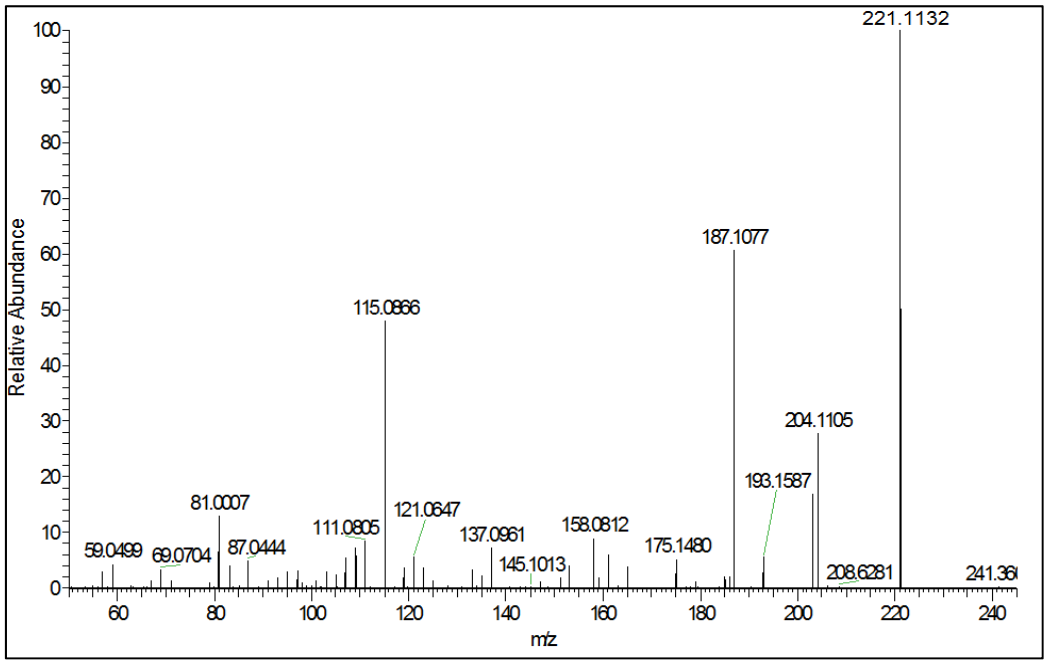

Fig. S20 MS^2 spectrum of CTR-TP8 (FTMS + p ESI Full ms2 221.12 @ hcd 40.00, RT 16.3 min).

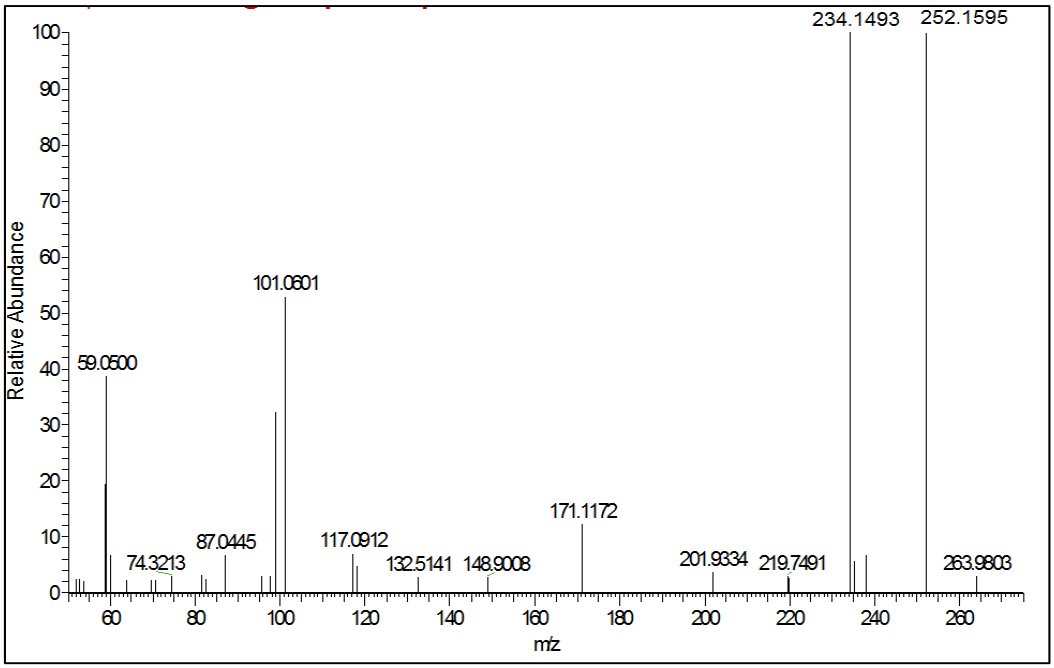

Fig. S21 MS^2 spectrum of FXF-TP3 (FTMS + p ESI Full ms2 252.16 @ hcd 10.00, RT 11.6 min).

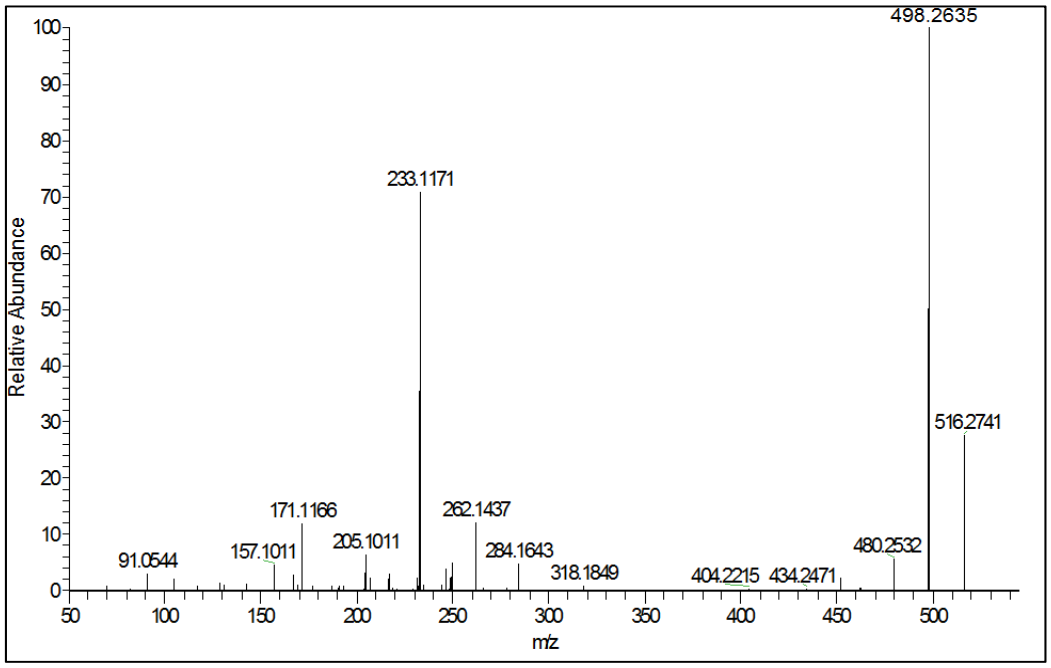

Fig. S22 MS^2 spectrum of FXF-TP4 (FTMS + p ESI Full ms2 516.28 @ hcd 25.00, RT 16.7 min).

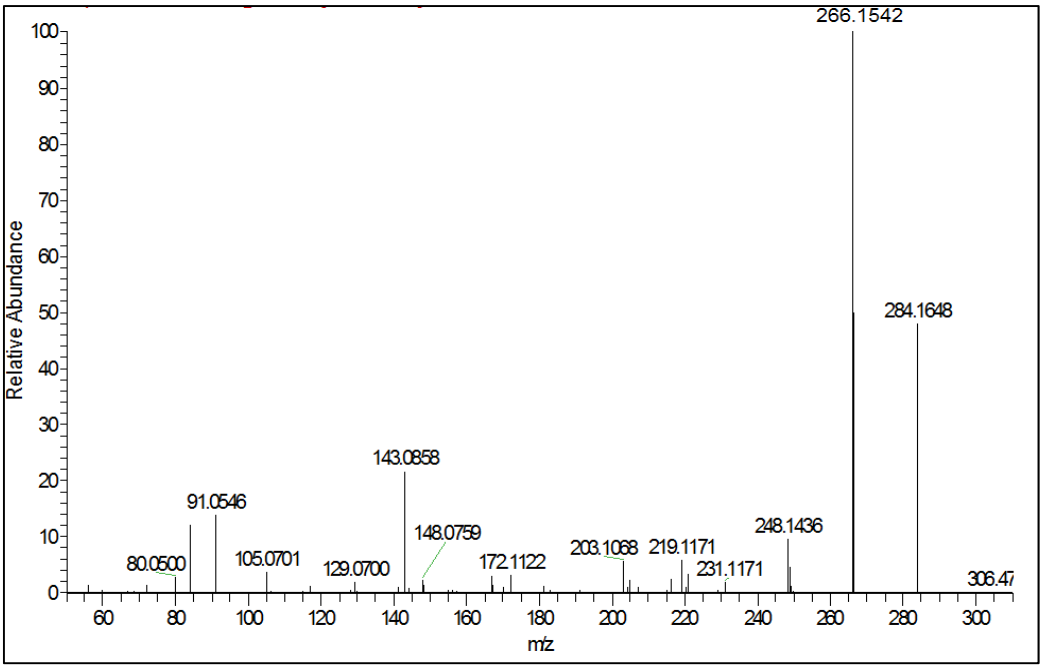

Fig. S23 MS^2 spectrum of FXF-TP5/6 (FTMS + p ESI Full ms2 284.16 @ hcd 25.00, RT 14.7 min).

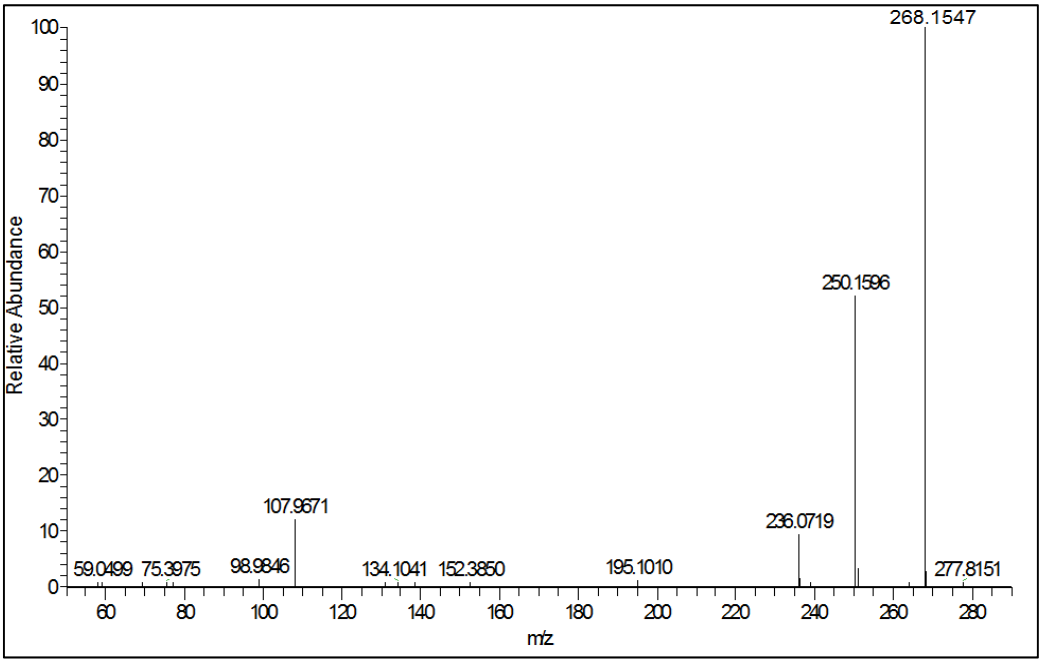

Fig. S24 MS^2 spectrum of FXF-TP7 (FTMS + p ESI Full ms2 268.17 @ hcd 10.00, RT 18.8 min).

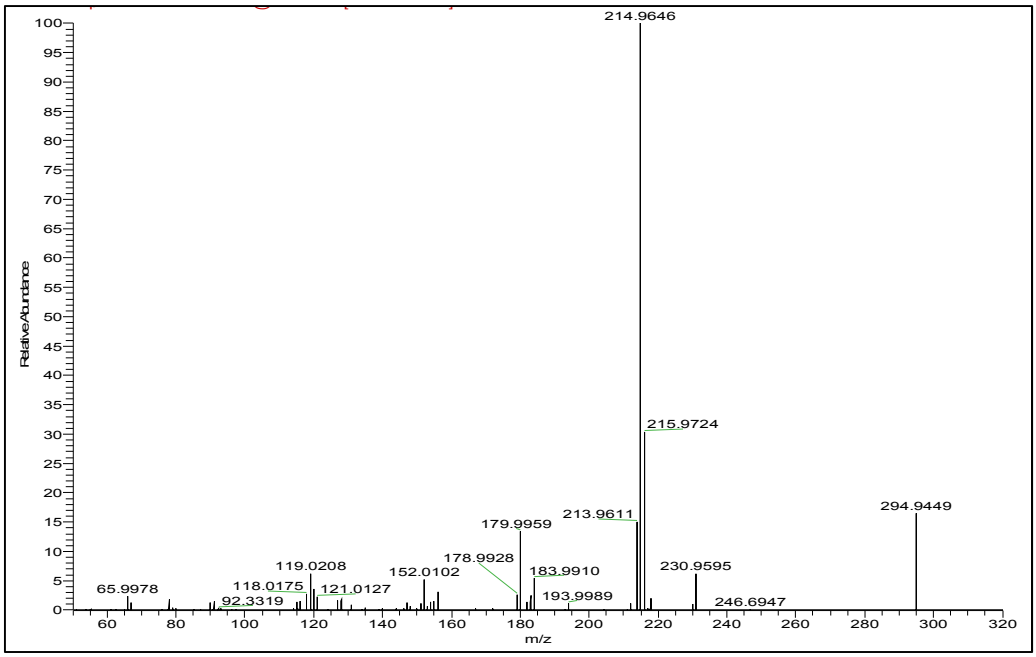

Fig. S25 MS^2 spectrum of HCTZ-TP2 (FTMS - p ESI Full ms2 294.94 @ hcd 40.00, RT 5.8 min).

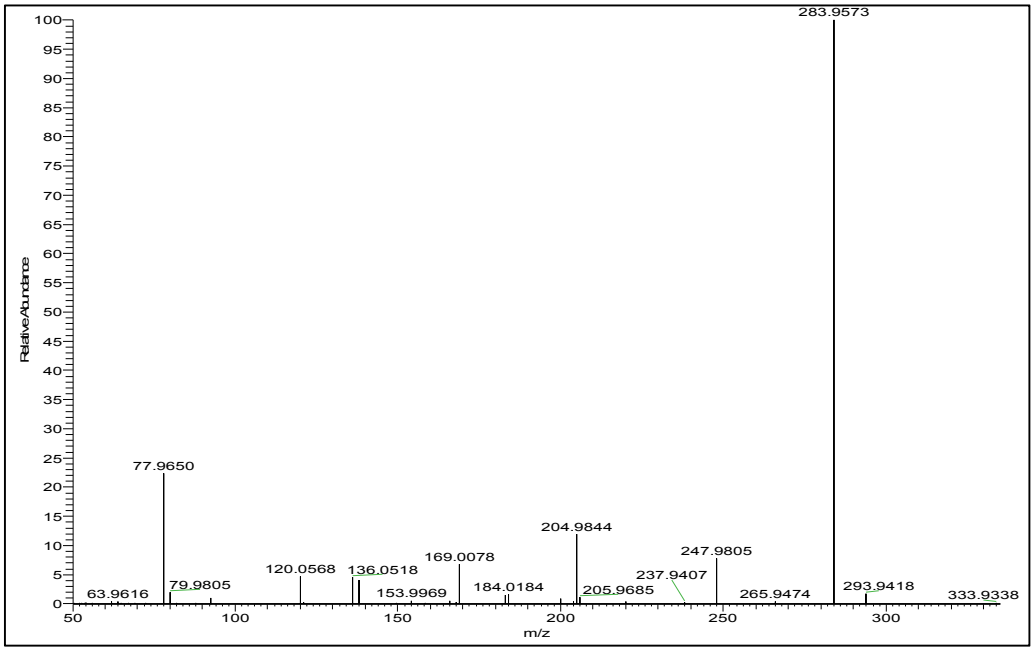

Fig. S26 MS^2 spectrum of HCTZ-TP3 (FTMS - p ESI Full ms2 311.95 @ hcd 40.00, RT 10.3 min).

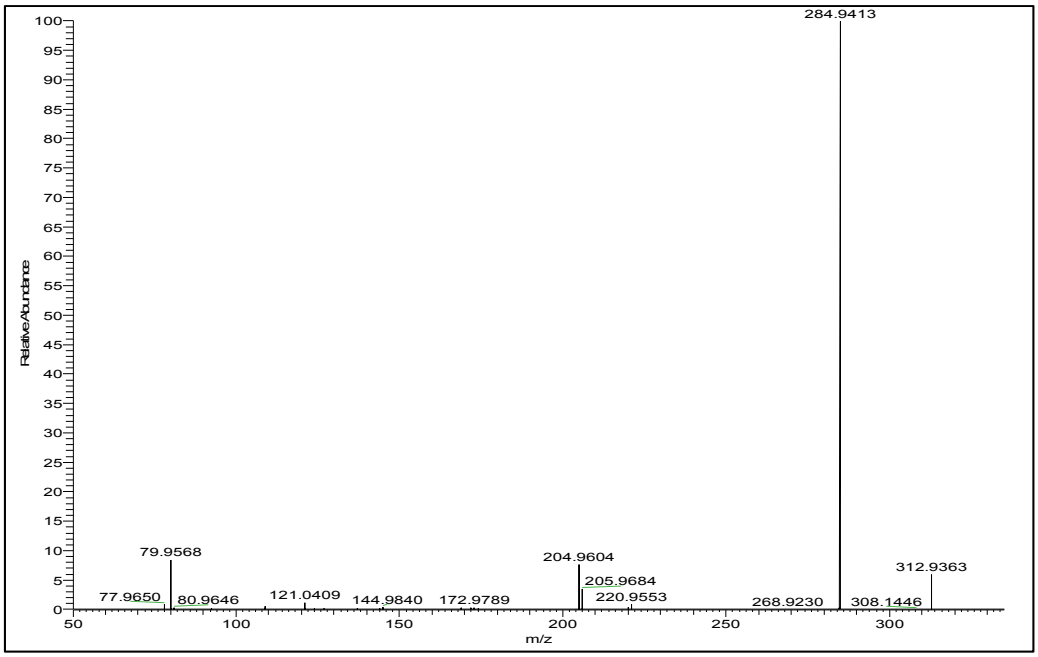

Fig. S27 MS2 spectrum of HCTZ-TP4 (FTMS - p ESI Full ms2 312.94 @ hcd 40.00, RT 9.8 min).

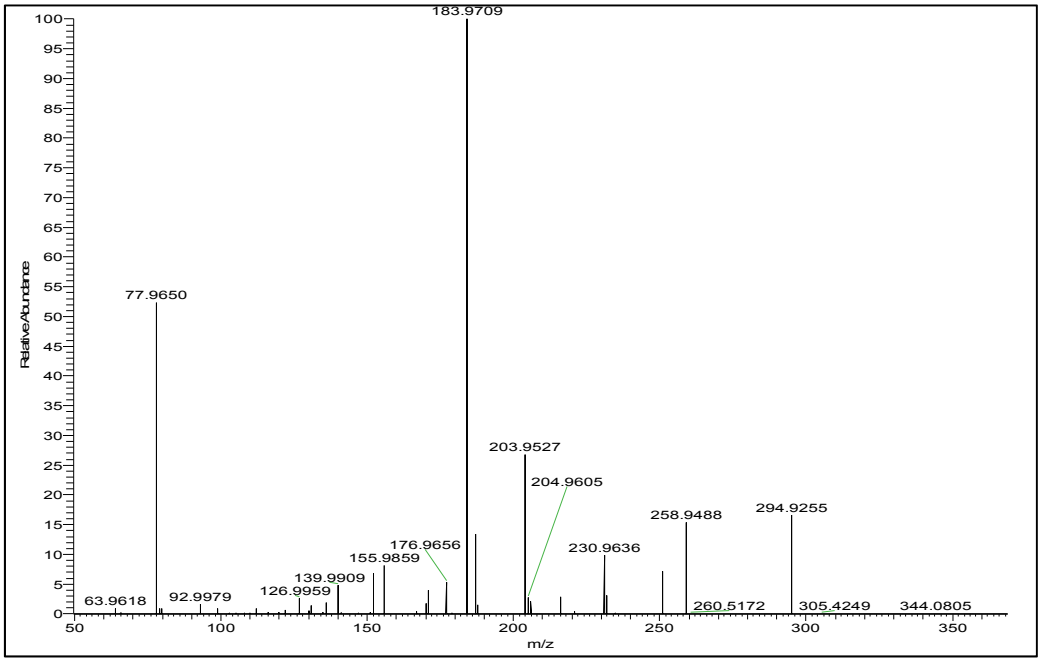

Fig. S28 MS^2 spectrum of HCTZ-TP5 (FTMS - p ESI Full ms2 341.93 @ hcd 40.00, RT 12.2 min).

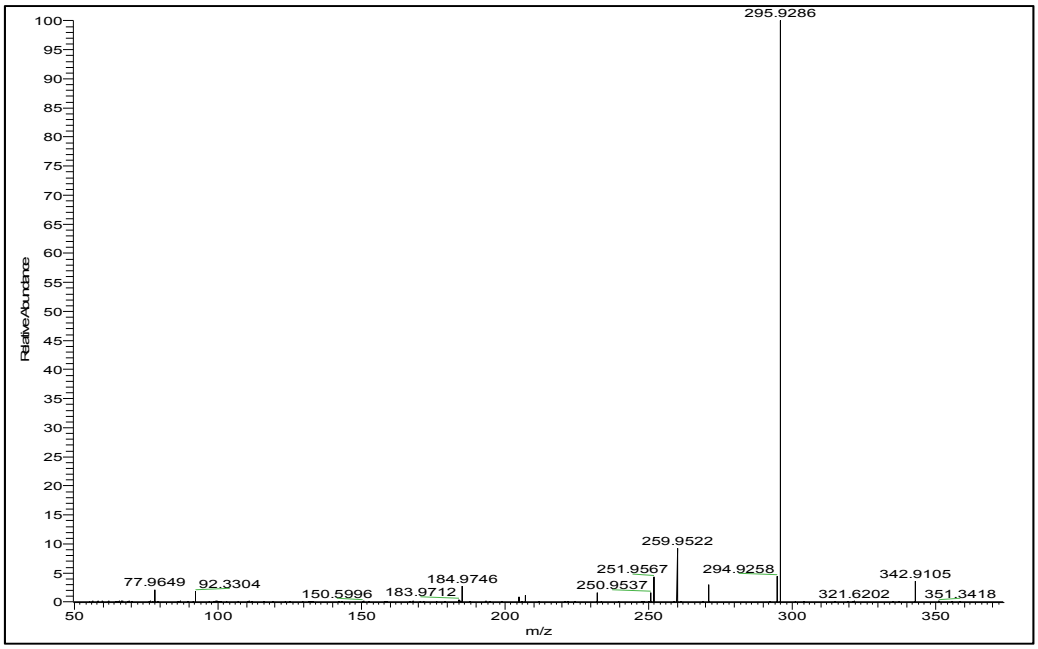

Fig. S29 MS^2 spectrum of HCTZ-TP6 (FTMS - p ESI Full ms2 342.91 @ hcd 20.00, RT 12.0 min).

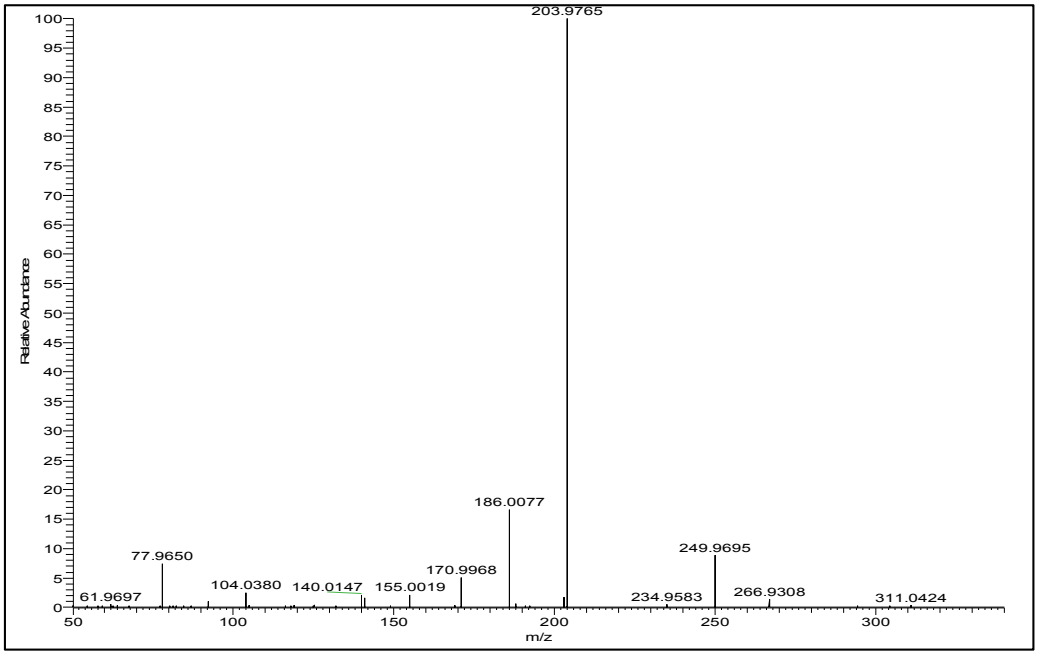

Fig. S30 MS^2 spectrum of HCTZ-TP7 (FTMS - p ESI Full ms2 313.93 @ hcd 40.00, RT 11.5 min).

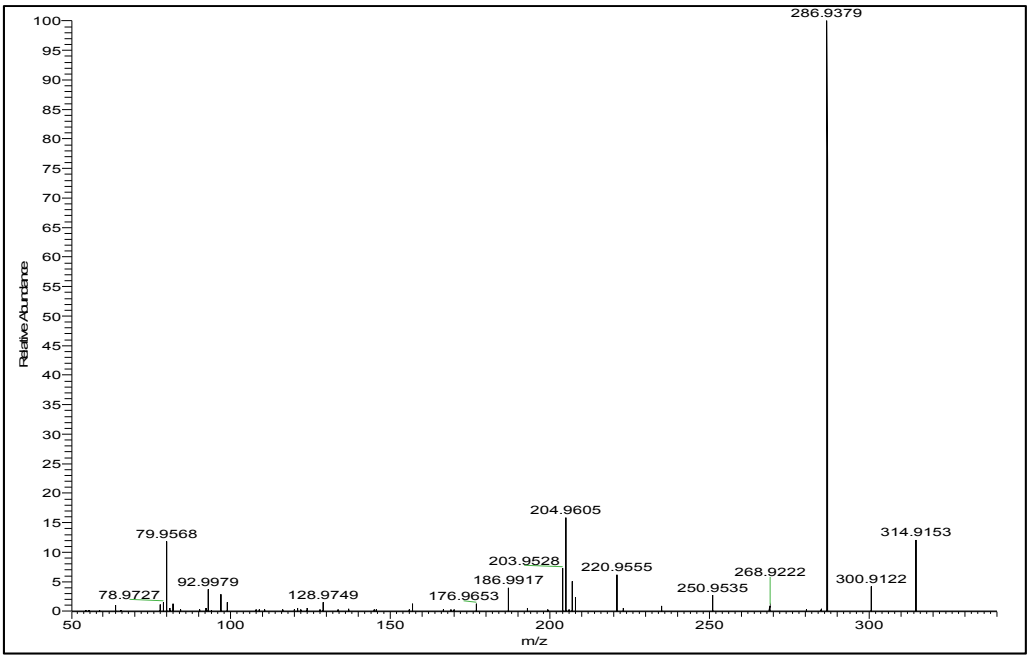

Fig. S31 MS^2 spectrum of HCTZ-TP8a (FTMS - p ESI Full ms2 314.92 @ hcd 40.00, RT 9.7 min).

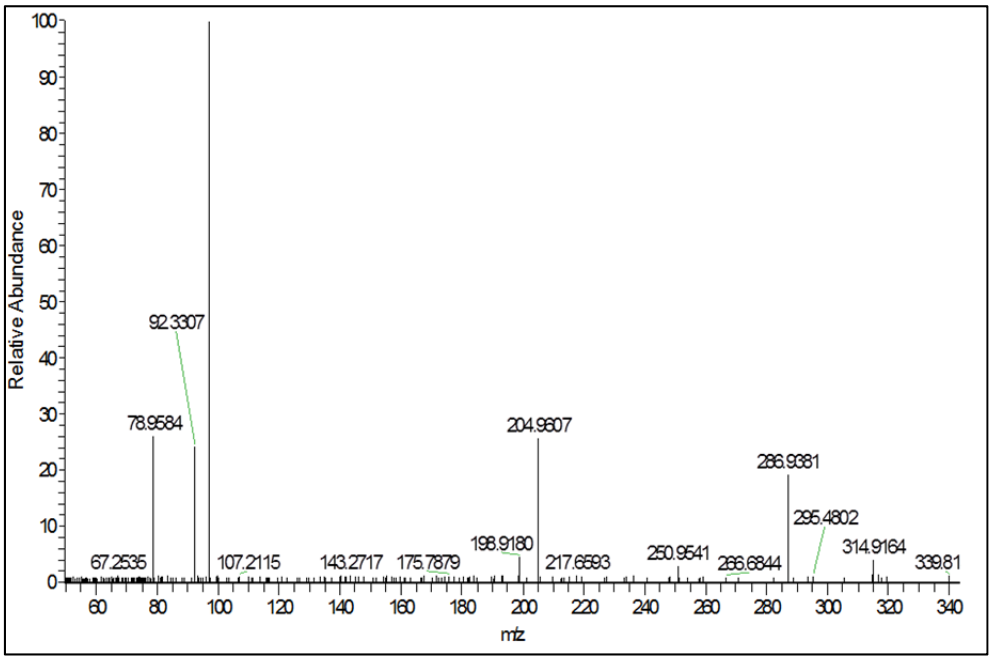

Fig. S32 MS^2 spectrum of HCTZ-TP8b (FTMS - p ESI Full ms2 314.92 @ hcd 40.00, RT 10.7 min).

REFERENCES

Bader, H., Hoigné, J., 1981. Determination of ozone in water by the indigo method. Water Res. 15(4), 449-456.

Escher B.I., Bramaz N., Mueller J. F. , Quayle P., Rutishauser S., Vermeirssen E. L. M., 2008. Toxic equivalent concentrations (TEQs) for baseline toxicity and specific modes of action as a tool to improve interpretation of ecotoxicity testing of environmental samples. J. Environ. Monit. 10, 612-621.

Hoigné, J., Bader, H. 1983a. Rate constants of reactions of ozone with organic and inorganic compounds in water—II: Dissociating organic compounds. Water Res. 17(2), 185-194.

Hoigné, J. and Bader, H. 1983b. Rate constants of reactions of ozone with organic and inorganic compounds in water—I: Non-dissociating organic compounds. Water Res. 17(2), 173-183.

Hoigné, J., Bader, H., 1994. Characterization of water quality criteria for ozonation processes. Part II: lifetime of added ozone. Ozone-Sci. Eng. 16(2), 121-134.

Huber, M.M., Canonica, S., Park, G.-Y., von Gunten, U., 2003. Oxidation of Pharmaceuticals during Ozonation and Advanced Oxidation Processes. Environ. Sci. Technol. 37(5), 1016-1024.

ISO 2007. Water quality - Determination of the inhibitory effect of water samples on the light emission of Vibrio fischeri (Luminescent bacteria test) - Part 3: Method using freeze-dried bacteria. EN ISO 11348-3.

Leitzke, A., Reisz, E., Flyunt, R., von Sonntag, C., 2001. The reactions of ozone with cinnamic acids: formation and decay of 2-hydroperoxy-2-hydroxyacetic acid. J. Chem. Soc., Perkin Trans. 2, 793-797.

Ming, X., Knight, B.M. and Thakker, D.R., 2011. Vectorial Transport of Fexofenadine across Caco-2 Cells: Involvement of Apical Uptake and Basolateral Efflux Transporters. Molecular Pharmaceutics 8(5), 1677-1686.

Muñoz, F., von Sonntag, C., 2000. Determination of fast ozone reactions in aqueous solution by competition kinetics. J. Chem. Soc., Perkin Trans. 2, 661-664.

Mvula, E., Naumov, S. and von Sonntag, C. (2009) Ozonolysis of Lignin Models in Aqueous Solution: Anisole, 1,2-Dimethoxybenzene, 1,4-Dimethoxybenzene, and 1,3,5-Trimethoxybenzene. Environ. Sci. Technol. 43(16), 6275-6282.

Mvula, E., von Sonntag, C. 2003. Ozonolysis of phenols in aqueous solution. Org Biomol Chem 1(10), 1749-1756.

Peter, A., von Gunten, U. 2007. Oxidation Kinetics of Selected Taste and Odor Compounds During Ozonation of Drinking Water. Environ. Sci. Technol. 41(2), 626-631.

Schymanski, E.L., Jeon, J., Gulde, R., Fenner, K., Ruff, M., Singer, H.P., Hollender, J. (2014) Identifying Small Molecules via High Resolution Mass Spectrometry: Communicating Confidence. Environ. Sci. Technol. 48(4), 2097-2098.

Tam, K.Y., Quere L., 2001. Multiwavelength spectrophotometric resolution of the micro-equilibria of cetirizine. Analytical Sciences 17(10), 1203-1208.

Theruvathu, J.A., Flyunt, R., Aravindakumar, C. T., von Sonntag C., 2001. Rate constants of ozone reactions with DNA, its constituents and related compounds, J. Chem. Soc., Perkin Trans. 2, , 269–274.

Yao D. C.C., Haag, W.R., 1991. Rate constants for direct reactions of ozone with several drinking water contaminants. Water Res. 25(7), 761-773.

Yasui-Furukori, N., Uno, T., Sugawara, K. and Tateishi, T., 2005. Different effects of three transporting inhibitors, verapamil, cimetidine, and probenecid, on fexofenadine pharmacokinetics. Clinical Pharmacology & Therapeutics 77(1), 17-23.

von Sonntag, C., von Gunten, U., 2012. Chemistry of Ozone in Water and Wastewater Treatment, IWA Publishing, London.